(2)

# NUMERICAL AND ANALYTICAL STUDIES OF STEFAN PROBLEMS.

# REPORT DOCUMENTATION PAGE

Form Approved
OMB No. 0704-0188



| 1. AGENCY USE ONLY (Leave blank) | 2. REPORT DATE | 3. REPORT TYPE AND DATES COVERED |
|---|---|---|
| | | FINAL 01 NOV 88 to 30 JUN 91 |

**4. TITLE AND SUBTITLE**
NUMERICAL AND ANAYLTICAL STUDES OF STEFAN PROBLEMS

**5. FUNDING NUMBERS**
F49620-89-C-0010
61102F 2304/A3

**6. AUTHOR(S)**
Milton E. Rose, Bolindra N, Borah, Robert E. White and Archimedes J. Kyrillidis

**7. PERFORMING ORGANIZATION NAME(S) AND ADDRESS(ES)**
North Carolin A&T State Univeristy
Office of Research Admin
Greensboro, NC 27411

**8. PERFORMING ORGANIZATION REPORT NUMBER**

**9. SPONSORING / MONITORING AGENCY NAME(S) AND ADDRESS(ES)**
AFOSR/NM
Bldg 410
Bolling AFB DC 20332-6448

**10. SPONSORING / MONITORING AGENCY REPORT NUMBER**
F49620-89-C-0010

**11. SUPPLEMENTARY NOTES**

**12a. DISTRIBUTION / AVAILABILITY STATEMENT**
Approved for public release; distribution unlimited.

**12b. DISTRIBUTION CODE**

**13. ABSTRACT** (Maximum 200 words)

Compact finite element scheme is used to solve Stefan Problem, with one-dimensional and two-dimensional numerically, using an enthaply formation. The numberical results indicate that the position of the melting front can be determined with first order accuracy by this method, the number of iterations at each time step being determined largely by the number of cells traversed by the front during a time step.

The codes both 1-D and 2-D Stefan problems are written in Cray Fortran and vectorization on the Cray Y-MP was used. The enthalpy formulation of the 1-D and 2-D Stefan problems are approximated by compact schemes. The numerical results are compared to known exponential solutions, and the solutions and errors are plotted using mathematica. Four paper have been published or completed for publication.

Three faculty members, Bolindra N. Borah (P.I.), Robert E. White (Co-P.I.), and Milton E. Rose (Co-P.I.) did work in this project. Besides three professors, there were three graduated students who also helped to complete the project.

**14. SUBJECT TERMS**

**15. NUMBER OF PAGES**

**16. PRICE CODE**

| 17. SECURITY CLASSIFICATION OF REPORT | 18. SECURITY CLASSIFICATION OF THIS PAGE | 19. SECURITY CLASSIFICATION OF ABSTRACT | 20. LIMITATION OF ABSTRACT |
|---|---|---|---|
| UNCLASSIFIED | UNCLASSIFIED | UNCLASSIFIED | SAR |

# NUMERICAL AND ANALYTICAL STUDIES OF STEFAN PROBLEMS

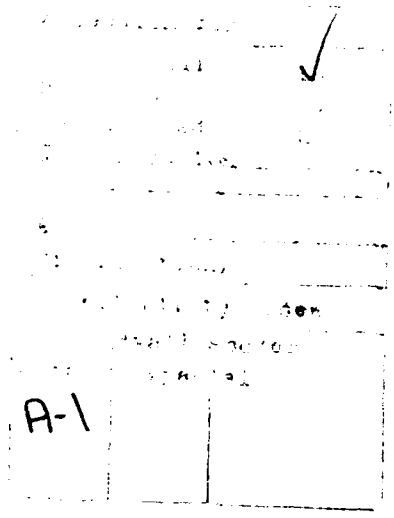


Dr. Milton E. Rose

Dr. Bolindra N. Borah
North Carolina A&T State University
Greensboro, NC

Dr. Robert E. White
North Carolina State University
Raleigh, NC

June 30, 1991

Air Force Office of Scientific Research
Bolling Air Force Base, D. C.

F49620-89-C-0010

North Carolina Agricultural and Technical
State University, Greensboro, NC

ECURITY CLASSIFICATION OF THIS PAGE

# REPORT DOCUMENTATION PAGE

Form Approved
OMB No. 0704-0188

| | |
|---|---|
| 1a. REPORT SECURITY CLASSIFICATION<br>Unclassified | 1b. RESTRICTIVE MARKINGS<br>NONE |
| 2a. SECURITY CLASSIFICATION AUTHORITY<br>NA | 3. DISTRIBUTION/AVAILABILITY OF REPORT<br>Distribution Unlimited |
| 2b. DECLASSIFICATION/DOWNGRADING SCHEDULE | |
| 4. PERFORMING ORGANIZATION REPORT NUMBER(S)<br>0002AA | 5. MONITORING ORGANIZATION REPORT NUMBER(S) |
| 6a. NAME OF PERFORMING ORGANIZATION<br>North Carolina A&T State University<br>6b. OFFICE SYMBOL (If applicable) | 7a. NAME OF MONITORING ORGANIZATION<br>Air Force Office of Scientific Research |
| 6c. ADDRESS (City, State, and ZIP Code)<br>Greensboro, NC 27411 | 7b. ADDRESS (City, State, and ZIP Code)<br>Building 410<br>Bolling AFB, D. C. 20332-6448 |
| 8a. NAME OF FUNDING/SPONSORING ORGANIZATION<br>NSAF, AFSC<br>8b. OFFICE SYMBOL (If applicable) | 9. PROCUREMENT INSTRUMENT IDENTIFICATION NUMBER<br>F49620-89-C-0010 |
| 8c. ADDRESS (City, State, and ZIP Code)<br>Building 410, Bolling AFB, DC 20332-6488 | 10. SOURCE OF FUNDING NUMBERS<br>PROGRAM ELEMENT NO. / PROJECT NO. 2304/A3 / TASK NO. / WORK UNIT ACCESSION NO. |

11. TITLE (Include Security Classification)

Numerical and Analytical Studies of Stefan Problems

12. PERSONAL AUTHOR(S)

Milton E. Rose, Bolindra N. Borah, Robert E. White, Archimedes J. Kyrillidis

| 13a. TYPE OF REPORT | 13b. TIME COVERED | 14. DATE OF REPORT (Year, Month, Day) | 15. PAGE COUNT |
|---|---|---|---|
| Final Report | FROM 11/1/88 TO 6/30/91 | | |

16. SUPPLEMENTARY NOTATION

| 17. COSATI CODES | | | 18. SUBJECT TERMS (Continue on reverse if necessary and identify by block number) |
|---|---|---|---|
| FIELD | GROUP | SUB-GROUP | |
| | | | |
| | | | |

19. ABSTRACT (Continue on reverse if necessary and identify by block number)

SEE ATTACHED SHEET

| | |
|---|---|
| 20 DISTRIBUTION/AVAILABILITY OF ABSTRACT<br>☐ UNCLASSIFIED/UNLIMITED ☐ SAME AS RPT. ☐ DTIC USERS | 21. ABSTRACT SECURITY CLASSIFICATION |
| 22a NAME OF RESPONSIBLE INDIVIDUAL | 22b. TELEPHONE (Include Area Code) / 22c. OFFICE SYMBOL |

# NUMERICAL AND ANALYTICAL STUDIES OF STEFAN PROBLEMS

## TABLE OF CONTENTS

# NUMERICAL AND ANALYTICAL STUDIES OF STEFAN PROBLEMS
FINAL Technical Report

ABSTRACT:

Compact finite element scheme is used to solve Stefan Problem, with one-dimensional and two-dimensional geometries numerically, using an enthalpy formation. The numerical results indicate that the position of the melting front can be determined with first order accuracy by this method, the number of iterations at each time step being determined largely by the number of cells traversed by the front during a time step.

The codes for both 1-D and 2-D Stefan problems are written in Cray Fortran and vectorization on the Cray Y-MP was used. The enthalpy formulation of the 1-D and 2-D Stefan problems are approximated by compact schemes. The numerical results are compared to known exponential solutions, and the solutions and errors are plotted using mathematica.

Four papers have been published or completed for publication. Three faculty members, Bolindra N. Borah (P.I.), Robert E. White (Co-P.I.), and Milton E. Rose (Co-P.I.) did work in this project. Besides three professors, there were three graduate students who also helped to complete the project.

1. A COMPREHENSIVE LIST OF THE OBJECTIVES OF RESEARCH EFFORT OR THE STATEMENT OF WORK:

This research aimed at developing

(1) Compact finite volume schemes for treating one and two dimensional Stefan Problems for bodies of general shapes and connectivities,

(2) Analytical approximations for the position of the interface in problems with cylindrical and spherical symmetry, and

(3) Development and testing of parallel algorithms for nector/ multiprocessing computers.

2. STATUS OF THE RESEARCH EFFORT: A substantive statement of significant accomplishments and progress towards achieving the research objectives

The compact finite volume method was used to treat general diffusion equations. By using intrinsic geometrical properties of the volume element, it was possible to describe discrete versions of the div, curl and grad operations which lead, using summation-by-parts techniques, to familiar energy equations as well as divcurl = 0 and curldiv = 0 identities. For the diffusion equations, these operators describe compact schemes whose convergence is assured by the energy equations and which yield both potential and flux vectors with second order accuracy. A simplified potential form is specially useful for obtaining numerical results by multigrid and ADI methods. The treatment of general curvilinear coordinates was shown to result from a application of these general results.

An implicit enthalpy scheme is used to solve one-dimensional and 2-D Stefan problems by compact finite volume scheme. The results are compared with known analytical solutions (exponential solution) and the solutions and the errors are plotted using Mathematica. Many intresting graphs are presented. Plot of the numerically calculated front positions and the least square fit for these numerically determined front positions are supplied. In two dimensional problems the 3-D plot of the numerical solution shows the behavior in the neighborhood of the front. A 3-D plot of the numerical error shows that the larger errors are mostly confined to the neighborhood of the front.

The 2-D Stefan Problem is solved for both Dirichlet and Neumann boundary conditions.

The parallel algorithms for the enthalpy formulation of multiple dimensional two phase Stefan problem have been studied. The compact scheme was shown to be adaptable to standard parallel algorithmic techniques for the efficient vectorization of multidimensional Stefan Problems.

The compact-ADI scheme for 2-D Stefan Problem was compared with compact SOR and traditional SOR method. Among all three method, compact-ADI scheme was found to be the most efficient method as regards to time of computation and memory usages. All three methods were computed in Alliant FX/40 and Cray Y-MP vector/multiprocessing computer. These results were scheduled to be published in paper (IV) listed in section 3.

3. A CUMULATIVE CHRONOLOGICAL LIST OF WRITTEN PUBLICATIONS IN TECHNICAL JOURNALS:

The following four papers are either published or ready for publication:

(i) Compact Finite Volume Methods for Diffusion Equations, Milton E. Rose, Journal of Scientific Computing, Vol. 4, No. 3, pages 261-290, Sept., 1989 (reprint enclosed).

(ii) An Implicit Enthalpy Scheme for One-phase Stefan Problems, Milton E. Rose, submitted for publication in the Journal of Scientific Computing (manuscript enclosed).

(iii) A Comparative Studies of Compact Volume Methods for the 2-D Diffusion Equation with Finite Difference ADI and SOR. Bolindra N. Borah, Robert E. White and Archimedes Kyrillidis.

(iv) A Compact Finite Volume Scheme for 2-D Stefan Problems and Vector/Multiprocessing Computers, Robert E. White, Bolindra N. Borah and Archimedes Kyrillidis (ready for publication, manuscript enclosed).

4. LIST OF PROFESSIONAL PERSONNEL ASSOCIATED WITH THE RESEARCH:

The following faculty members have worked in this project:

(i) Bolindra N. Borah, Professor of Applied Mathematics and Computer Science (P.I.), North Carolina A&T State University, Greensboro, NC.

(ii) Milton E. Rose, Adjunct Professor of Mathematics and Computer Science (Co-P.I.), North Carolina A&T State University, Greensboro, NC.

(iii) Robert E. White (Consultant) Professor of Mathematics, North Carolina State University, Raleigh, NC.

The following graduate students have worked in this projects:

(i) Mr. Nader Nassim-Sobhan, received the M. S. degree in Applied Mathematics, Summer 1989, now employed by IBM in New York.

(ii) Miss Oi M. Foong, received the M. S. degree in Applied Mathematics, Summer 1990, now working at the University of Singapore as a systems analyst.

(iii) Mr. Archimedes Kyrillidis, will be completing the M. S. in Applied Mathematics, Summer 1991, will enter North Carolina State in Raleigh, NC and begin work on the Ph.D. degree.

5. INTERACTIONS: PAPER PRESENTED AT MEETINGS, CONFERENCES, SEMINARS, ETC.

(i) The paper entitled "A Compact ADI Scheme for 2-D Stefan Problems and Vector/Multiprocessing Computers" will be presented at the Second International Conference on Industrial and Applied Mathematics, July 8-12, 1991 to be held at Washington, D. C.

(ii) The entire research findings were presented at the seminar organized by the McDonnell Douglas Aircraft Company, St. Louis, MO, 63166 held April 23, 24, 1991.

ATTACHMENT #1

Reprinted from JOURNAL OF SCIENTIFIC COMPUTING

Vol. 4, No. 3, September 1989
*Printed in Belgium*

# Compact Finite Volume Methods for the Diffusion Equation

**Milton E. Rose**[1]

*Received September 21, 1989*

We describe an approach to treating initial-boundary-value problems by finite volume methods in which the parallel between differential and difference arguments is closely maintained. By using intrinsic geometrical properties of the volume elements, we are able to describe discrete versions of the div, curl, and grad operators which lead, using summation-by-parts techniques, to familiar energy equations as well as the div curl = 0 and curl grad = 0 identities. For the diffusion equation, these operators describe compact schemes whose convergence is assured by the energy equations and which yield both the potential and the flux vector with second-order accuracy. A simplified potential form is especially useful for obtaining numerical results by multigrid and ADI methods. The treatment of general curvilinear coordinates is shown to result from a specialization of these general results.

**KEY WORDS:** Finite volumes; compact schemes; elliptic; diffusion equation; curvilinear coordinates.

## 1. INTRODUCTION

Let $V$ be a domain with boundary surface $S$ on which $\mathbf{n}$ is the outward unit normal. This article describes a finite volume scheme for solving the diffusion equation for a *potential* $\phi$ and *flux* $\mathbf{u}$ in the form

D.E. $$\phi_t = \operatorname{div} \mathbf{u} - f \qquad \text{in } V \tag{1.1}$$

$$\operatorname{grad} \phi = \mathbf{u}$$

B.C. $$\alpha \mathbf{u} \cdot \mathbf{n} + \beta \phi = g \qquad \text{on } S, \qquad t \geqslant 0 \tag{1.2}$$

I.C. $$\phi = g_0 \qquad \text{in } V, \qquad t = 0 \tag{1.3}$$

[1] Department of Mechanical Engineering, N.C. A & T State University, Greensboro, North Carolina 27411. Present Address: 4505 Tower Road, Greensboro, North Carolina 27410.



0885-7474/89/0900-0261$06.00/0 

in both the steady and unsteady cases. We recall that the solution of this problem satisfies an "energy" equation

$$\frac{d}{dt}\int_V \phi^2\, dV + \int_V \mathbf{u}\cdot\mathbf{u}\, dV = \int_S \phi\mathbf{u}\cdot d\mathbf{S} - \int_V \phi f\, dV \tag{1.4}$$

which follows by multiplying the first equation in (1.1) by $\phi$ and integrating by parts. We also recall that when $f=0$ the maximum–minimum values of $\phi$ either lie on the boundary $S$ or, in case $t=0$, in $V$ itself.

A discrete form of these results will hold for the finite volume scheme and includes results about generalized curvilinear coordinate mappings as a special case. We will identify finite volume operators $\mathrm{div}_h$, $\mathrm{grad}_h$, and $\mathrm{curl}_h$ which are consistent with their differential counterparts and from which a discrete energy expression corresponding to (1.4) will follow by simple summation-by-parts identities. The important identities $\mathrm{div}_h\,\mathrm{curl}_h = 0$ and $\mathrm{curl}_h\,\mathrm{grad}_h = 0$ will also remain valid, as we will show at a later point in the article. A potential form involving the operator $\mathrm{div}_h\,\mathrm{grad}_h\,\phi$, which is obtained by eliminating $\mathbf{u}$, leads to a symmetric, positive definite operator to which multigrid and other fast solution techniques are applicable.

The fact that the finite volume schemes described here lead to discrete energy expressions is the principal result of this article. It ensures that the schemes converge. We will also find that the approximations to *both* $\phi$ and $\mathbf{u}$ will be second order accurate. This result is similar to that obtained for mixed finite element methods (Brezzi, 1988; Strang and Fix, 1973) and it is possible, in fact, to view the present scheme as a finite element method that involves nonconforming elements (Gatski *et al.*, 1989; Lustman and Rose, 1988).

Many of these ideas can be illustrated most simply for steady, one-dimensional problems, for which reason we first discuss the equations $\phi' = \mathbf{u}$, $\mathbf{u}' = f$ in detail. We will find it natural to introduce a *primary mesh*, which is formed by the end points of subintervals into which the basic domain is divided, and a *dual mesh*, which is formed by the center points of the primary mesh. The variables $\phi$ and $\mathbf{u}$ will be associated with the primary mesh while another variable $\psi$ will be associated with the dual mesh. An algebraic relationship between $\phi$, $\psi$, and $\mathbf{u}$ on each subinterval provides an approximation to the solution operator (for which reason the scheme is called *compact*) and the solution in the large is obtained by imposing continuity conditions for $\phi$ and $\mathbf{u}$ at points of the primary mesh. Both $\phi$ and $\psi$ will be found to converge with second-order accuracy to the solution at the points at which they are defined. Furthermore, as noted above, although $\mathbf{u}$ will be defined by one-sided divided differences involving

$\phi$ and $\psi$, its convergence will also be second order accurate as a result of the continuity conditions imposed.

In extending these ideas to higher-dimensional problems by subdividing the solution domain $V$ into volume elements we will also find that a primary and dual grid play a natural role. Now the variables $\phi$ and $\mathbf{u}$ will be associated with the center points of the faces of a volume element while $\psi$ will be associated with the center of the element. However, an additional variable $\zeta$ (or a box-variable $\chi$) which is associated with the edges (vertices) of the element will also be required. The compact scheme will describe relationships between these variables which produce second-order accurate results at the points indicated. In the method discussed here, the nontangential components of $\mathbf{u}$ on a face of an element are obtained with the use of one-sided differences in terms of $\phi$ and $\psi$ while its tangential components are determined solely by the edge values $\zeta$, and these are obtained in terms of $\psi$ at points of the dual grid by bilinear interpolation. In the case of (uniform or nonuniform) Cartesian or orthogonal coordinate elements, the variables $\zeta$ as well as the tangential components of $\mathbf{u}$ on faces of elements can be obtained by postprocessing, if required.

Some of these ideas are familiar from applications of finite volume methods to fluid dynamics and are described in Peyret and Taylor (1983) and in a review paper by Vinokur (1989). A focus of many such methods is on the treatment of conservation laws for fluids. As noted by these authors, the primary and dual grids often play a role in many such schemes whenever gradient terms are included, as occur when viscous effects arise. Indeed, the need to accurately approximate quantities like the stress tensor at boundaries of general domains is a principal reason to resort to finite volume methods, although their use may add significantly to the cost of computations. To understand some of the problems that can arise, the diffusion equation can serve as a useful model. We will find that the relationships between grid variables differ in important respects from those described elsewhere. Many schemes place primary emphasize on the vertex (box) variables and most methods deliberately avoid the use of one-sided differencing to approximate the flux except, perhaps, at boundaries. Although compact schemes related to those described here have been used for Cartesian grids, e.g., Gatski *et al.* (1989) and Rose (1983), the roles of the variables were not completely developed.

The paper concludes by describing the rather straightforward modifications that are required to treat the time-dependent problem. The result is a Crank–Nicholson-type scheme and energy arguments provide convergence estimates for the finite volume method. We are also able to show that energy arguments can be adapted to a Peaceman–Rachford ADI scheme.

## 2. STEADY ONE-DIMENSIONAL PROBLEMS

### 2.1. Notations

On an interval $[1_-, 1_+]$ consider the problem:

D.E. $$u' = f \qquad (2.1a)$$

$$\phi' = u$$

B.C. $$\phi = g \qquad \text{for} \quad x = 1_\pm \qquad (2.1b)$$

The associated energy equation is

$$\int \phi f \, dx + \int u^2 \, dx = (\phi u)_{1_+} - (\phi u)_{1_-} \qquad (2.2)$$

Divide $[1_-, 1_+]$ into $M$ nonoverlapping subintervals $I_j \equiv \{x \mid x_{j-1/2} \leqslant x \leqslant x_{j+1/2}\}$ with center points $x_j$, $j = 1/2, 3/2, \ldots, M - 1/2$. The points $x_j$, $j = 1, 2, \ldots, M-1$, are end points of the subintervals which lie interior to $[1_-, 1_+]$. We let $I_e$, $I_c$ denote the sets of indices corresponding to these points:

$$I_e = \{1, 2, \ldots, M-1\} \qquad \text{(interior end points)}$$

$$I_c = \{1/2, 3/2, \ldots, M-1/2\} \qquad \text{(center points)}$$

We adopt the finite-difference notations $\Delta x_i = x_{i+1/2} - x_{i-1/2}$, $h_i = \Delta x_i/2$, $\mathbf{u}(x_i) = u_i$. By introducing the central average and difference operators

$$\mu\phi_j \equiv (\phi_{j+1/2} + \phi_{j-1/2})/2, \qquad \Delta\phi_j \equiv (\phi_{j+1/2} - \phi_{j-1/2}) \qquad (2.3)$$

we can verify the summation-by-parts identities

$$\Delta(\phi\psi) = (\mu\phi)(\Delta\psi) + (\Delta\phi)(\mu\psi) \qquad (2.4a)$$

$$\mu(\phi\psi) = (\mu\phi)(\mu\psi) + (\Delta\phi)(\Delta\psi)/4 \qquad (2.4b)$$

Both will play a central role in establishing energy results.

### 2.2. A Compact Scheme

In each subinterval $I_j$, construct an approximate solution using values $\phi_{j\pm 1/2}$ as boundary data. Specifically, (i) for $j \in I_c$ set

$$\Delta u_j \equiv u_{j+1/2} - u_{j-1/2} = \Delta x_j f_j \qquad (2.5)$$

$$h_j u_{j+1/2} = (\phi_{j+1/2} - \psi_j) \qquad (2.6a)$$

$$h_j u_{j-1/2} = (\psi_j - \phi_{j-1/2}) \qquad (2.6b)$$

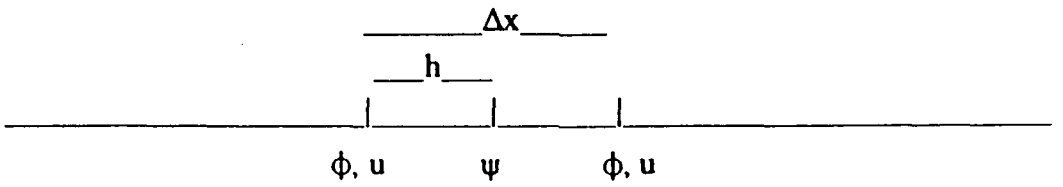


**Fig. 1.** An interval showing the association of the variables $\phi, u$ with its end points and of $\psi$ with its center point.

Adopting the convention that $\psi_j$ *indicates an approximation to the potential solution at the center of the interval, while* $\phi_{j\pm 1/2}$ *indicates the approximation as its end points* we see that (2.5) is a central difference approximation to $\mathbf{u}' = f$, while (2.6) approximates $\phi' = u$ by one-sided differences. Then Eqs. (2.5) and (2.6) can be solved for $u_{j\pm 1/2}$ and $\psi_j$ in each interval in terms of $\phi_{j\pm 1/2}$ considered as boundary data.

(ii) Next, require that both $u$ and $\phi$ shall be *continuous across every end point* common to two intervals, i.e.,

$$[u]_i = [\phi]_i = 0 \qquad \text{for} \quad i \in I_e \text{ (end points)} \tag{2.7}$$

(This is implied by our notation, since we have not distinguished between the right- and left-hand limits of $u$ and $\phi$ at end points.) Using (2.6) to evaluate $u_{i+1/2}$ at the right and left end points of the adjacent intervals $I_{i-1/2}, I_{i+1/2}$ we find

$$\Delta x_{i+1/2} u_{i+1/2} = (\psi_{i+1} - \psi_{i-1}), \qquad i \in I_e \tag{2.8}$$

which indicates that the accuracy of $u$ may be higher than that suggested by the one-sided difference expressions which originally defined $u$ in (2.6). Also note that (2.6) can be used to express the continuity condition $[u]_i = 0$ in terms of $\phi, \psi$ with the result

$$(\phi_i - \psi_{i-1/2})/h_{i-1/2} = (\psi_{i+1/2} - \phi_i)/h_{i+1/2} \tag{2.9a}$$

and which, in the case of equal intervals, reduces to

$$\phi_i = \mu\psi_i, \qquad i \in I_e \text{ (end points)} \tag{2.9b}$$

The addition of the boundary conditions leads to a determined system of algebraic equations for the $M$ values of $\psi$ and the $M+1$ values of $\phi$ and $u$.

The special nature of this system is worth noting. By eliminating $u$ from (2.5) using (2.6) we find, in the case of equal intervals,

$$(\mu\phi_i - \psi_i) = 2h^2 f, \qquad i \in I_c \text{ (center points)} \tag{2.10a}$$

and if we also write the continuity conditions (2.9b) in the form

$$(\mu\psi_i - \phi_i) = 0, \qquad i \in I_c \text{ (end points)} \tag{2.10b}$$

it is evident that $\phi_i$, $\psi_i$ are the odd-even components of the solution vector of a tridiagonal system of equations which is, thus, easily solved. In sharp contrast to (2.10), the standard finite difference scheme for solving (2.1) is

$$(\mu\phi_i - \psi_i) = h^2 f_i, \qquad i \in I_c \cup I_c \tag{2.10c}$$

so that some differences with standard numerical treatments of differential equations are to be expected using the schemes considered in this article.

### 2.3. The Energy Equation and Convergence

We will now show that this scheme leads to a discrete form of the energy equation (1.4). For simplicity, we will assume a uniform mesh. Add and subtract the expressions

$$(\Delta x/2)\, u_{j\pm 1/2} = \pm(\phi_{j\pm 1/2} - \psi_j)$$

given in (2.6) to obtain

$$\Delta x\, \mu u_j = \Delta\phi_j \tag{2.11a}$$

$$\psi_j = \mu\phi_j - \Delta x\, \Delta u_j/4 \tag{2.11b}$$

and we see that the approximations to $\phi$ and $\psi$ *are second order with respect to the center of an interval.* Then, starting with

$$\Delta u_j = \Delta x\, f_j \tag{2.5}$$

multiply by $\psi$ and use (2.11) and (2.4) to obtain

$$\begin{aligned}
\psi\, \Delta u &= (\mu\phi - (\Delta x/4)\, \Delta u)\cdot \Delta u \\
&= \Delta(\phi u) - (\mu u\, \Delta\phi + (\Delta x/4)(\Delta u)^2) \\
&= \Delta(\phi u) - \Delta x[(\mu u)^2 + (\Delta u)^2/4] \\
&= \Delta(\phi u) - \Delta x\, \mu(u^2)
\end{aligned} \tag{2.12}$$

(Here and in the following we omit subscripts when no confusion is likely to arise.) Summing over *center points* of intervals we obtain

$$\sum_{I_c} (\psi_j\, \Delta u_j + \Delta x\, \mu u_j^2) = (\phi u)\Big|_1^{I_+} - \sum_{I_c} [\phi u]_i$$

Because of the continuity conditions, the jumps [ ] vanish and we obtain the discrete energy expression

$$\sum_{I_c} (\psi_j f_j + \mu u_j^2)\, \Delta x = (\phi u)\Big|_1^{I_c} \tag{2.13}$$

This result will enable us to conclude that $\phi$, $\psi$, and $u$ converge with second-order accuracy. Introduce center-point and end-point norms as follows:

$$\|\psi\|_c = \left(\sum_{I_c} \psi_j^2\, \Delta x\right)^{1/2} \tag{2.14a}$$

$$\|u\|_e = \left[\left(u_0^2 + u_M^2 + \sum_{I_c} u_j^2\right) \Delta x\right]^{1/2} \tag{2.14b}$$

By summing (2.8) and using (2.6) we find

$$\psi_{j+1} - \phi_0 = \tfrac{1}{2} u_0 + \sum_{I_c} u_i$$

and if we also assume end-point conditions $\phi_0 = \phi_M = 0$ we obtain the inequality

$$\|\psi\|_c \leqslant C\, \|u\|_e$$

The energy expression itself leads to the estimate

$$\|u\|_e^2 \leqslant \|\psi\|_c\, \|f\|_c$$

while the continuity condition (2.9) results in

$$\|\phi\|_e \leqslant \|\psi\|_c$$

Thus, we have

$$\begin{aligned} \|\psi\|_c &\leqslant C^2\, \|f\|_c \\ \|\mathbf{u}\|_e &\leqslant C\, \|f\|_c \\ \|\phi\|_e &\leqslant C^2\, \|f\|_c \end{aligned} \tag{2.15}$$

Applying this to the homogeneous problem we conclude that $u = \phi = \psi = 0$. Thus the algebraic problem has a solution that is unique. Next, interpreting $f$ as the truncation error, we have $f = O(\Delta x^2)$, and we see that $\phi$, $\psi$, and $u$ converge with second-order accuracy.

This conclusion about the second-order accuracy of $u$ applies not only to its values at interior end points, as might be expected from (2.8), but

**Table I.** Error Norms

| Number of intervals | $\|\phi_{error}\|_e$ | $\|u_{error}\|_e$ |
|---|---|---|
| 6 | 1.234*e*-2 | 1.851*e*-2 |
| 12 | 3.472*e*-3 | 9.259*e*-3 |
| 24 | 8.680*e*-4 | 2.893*e*-3 |
| 48 | 2.170*e*-4 | 7.957*e*-4 |
| 96 | 5.425*e*-5 | 2.080*e*-4 |
| 192 | 1.356*e*-5 | 5.312*e*-5 |

also to the values $u_0$ and $u_M$ at the end points of $[1_-, 1_+]$ itself and which, we recall, were defined in Eq. (2.6) by one-sided difference expressions.

Table I presents computations which verify these conclusions for the differential equation (2.1) corresponding to the solution $\phi = x^2(1-x)^2$. Note that the errors are measured at the end points of intervals.

Finally, we remark that more general boundary conditions involving both $u$ and $\phi$ also lead to the same conclusions.

## 2.4. The Potential Form

By eliminating the flux $u$ in (2.1) we obtain the familiar second-order equation $\phi'' = f$ which we call the *potential* form. The difference scheme that corresponds to this may be obtained by eliminating $u$ in the scheme just described. To illustrate, using (2.6), eliminate $u$ in

$$\Delta u_j = \Delta x\, f_j \tag{2.5}$$

to obtain

$$\begin{aligned} h^2 f_j &= (\mu\phi_j - \psi_j), \qquad j \in I_e \\ h &= \Delta x/2 \end{aligned} \tag{2.16}$$

As we have seen, for uniform meshes the continuity conditions $[\mathbf{u}] = 0$ result in

$$\phi_i = \mu\psi_i, \qquad i \in I_e \tag{2.9b}$$

To these are to be added the boundary conditions

$$\phi_0 = g_-, \qquad \phi_M = g_+$$

When $f = 0$ we obtain

$$\psi = \mu\phi, \qquad \phi = \mu\psi \tag{2.17}$$

and the maximum–minimum property of the solution is an immediate consequence. This can be used to develop an alternate proof of convergence.

The potential form for the discrete problem can be seen to arise as a variational problem associated with the discrete energy equation. The maximum–minimum property reflects the fact that the associated algebraic problem is symmetric and positive definite. In the general treatment, the potential form will be more suitable for numerical work, while the general form involving $\phi$, $\psi$, and $u$ as a first-order system will prove more convenient for theoretical discussions, particularly for the development of energy estimates.

## 3. A COMPACT FINITE-VOLUME METHOD

We now turn to the problem of treating the boundary value problem corresponding to the steady-state solution of (1.1) when $V$ is a general volume. Our objective will be to partition $V$ into volume elements $\delta V$ in such a manner that the prescribed boundary data on $S$ can be accurately transmitted to the boundary elements and then, by solving a discrete boundary value problem in each element corresponding to a compact scheme, obtain an approximate solution in all elements which also satisfies an energy expression, thus ensuring convergence. As a result, we expect to be able to treat problems posed in curvilinear coordinates as a special, but important, case.

In order to be able to generalize the arguments given earlier, a number of additional notations will have to be introduced. Before doing so, we will first present a short overview of the principal ideas that will be involved. The more detailed discussion and demonstration that the final result again leads to an energy expression and thus produces a convergent scheme may be omitted if the reader wishes to turn to the discussion of the time-dependent problem given in Section 4.

### 3.1. An Overview

Guided by the earlier discussion of the one-dimensional problem, we may identify the following requirements to construct a discrete approximation to $\operatorname{div} \mathbf{u} = f$, $\mathbf{u} = \operatorname{grad} \phi$ when volume elements are involved:

i. Construct consistent, discrete approximations to $\operatorname{div} \mathbf{u}$, $\operatorname{grad} \phi$ in a volume element $\delta V$ in terms of variables associated with $\mathbf{u}$ and $\phi$ at appropriate points of $\delta V$.

ii. Further relate these variables as may be required so as to lead to a determined and consistent system of algebraic equations from which **u** and $\phi$ can be determined whenever boundary conditions are prescribed on $S$.

iii. Develop a difference calculus that allows summation-by-parts identities to be applied to volume elements and thereby lead to a discrete energy expression from which a convergence argument can be constructed.

We will confine our attention to hexahedral volume elements $\delta V$, although we will allow certain of its vertices to coalesce, thereby including tetrahedra and related elements in our discussion. Figure 2 indicates the center point $P$ of $\delta V$, the center $Q$ of an oriented face $\delta$S, and a representative center point $R$ of an edge of $\delta$S on which $T$ is a vertex. In addition to the variables $\phi(Q)$, $\psi(P)$ introduced in our discussion of the one-dimensional problem, we will also associate another variable $\zeta(R)$ with points $R$. These variables will approximate the potential solution at the points indicated. Later, we will also associate a variable $\chi$ with the vertex points $T$. Section 3.2 introduces notations that allow us to describe various geometrical properties of an element and from which averaging and difference operators, corresponding to (2.4), can be introduced.

Section 3.3 describes discrete approximations to the operators div and grad. The approximation to div **u** is based on the use of Gauss' theorem in a volume element. Center-point quadrature approximations to the surface integrals involved leads to a discrete operator $\text{div}_h$ which provides an intrinsically consistent, second-order accurate, approximation to div **u** in terms of the normal components of **u** at center points of faces $\delta$S. This is

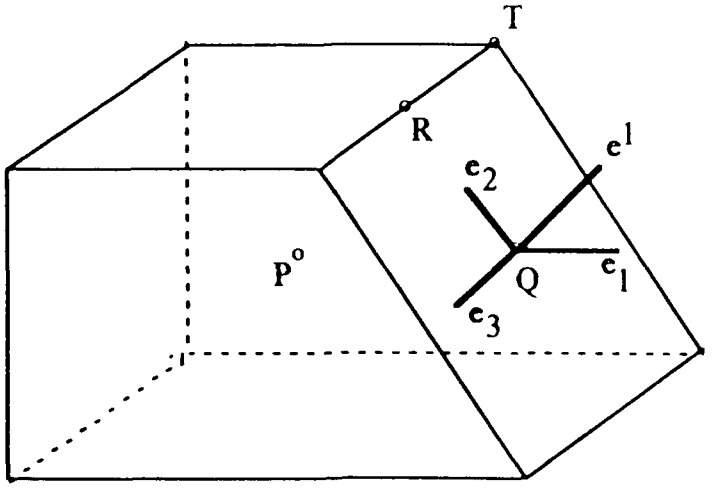


**Fig. 2.** A normal volume element; $P$, $Q$, $R$, are the centers of the volume $\delta V$, a face $\delta$S, and an edge on which $T$ is a vertex. Shown at $Q$ is a basis $[e]$ and $e^1$, the unit normal to $\delta$S.

a familiar idea in finite volume methods. An approximation to $\mathbf{u} = \text{grad}\,\phi$ will result from the integral form

$$\int_C \mathbf{u} \cdot d\mathbf{x} = \phi(B) - \phi(A)$$

in which the points $A$ and $B$ are identified with the points $P$, $Q$, and $R$ in Fig. 2. A midpoint evaluation of the integral will determine two tangential components of $\mathbf{u}$ lying in a surface element in terms of the variable $\zeta$ at edges of $\delta\mathbf{S}(Q)$. The remaining nontangential component of $\mathbf{u}$ on $d\mathbf{S}$ will result by using points $P$ and $Q$ and a one-sided evaluation of the integral at $Q$. This approximation will lead to second-order accuracy as a result of imposing additional continuity conditions for the variables on $\delta\mathbf{S}$, as occurred in the one-dimensional case. We indicate by $\text{grad}_h\,\phi$ the vector $\mathbf{u}$ evaluated at each face using this construction.

The compact scheme which emerges is described in Section 2.4 and can be summarized as follows:

a. In each element $\mathbf{u}$, $\phi$, $\psi$, $\zeta$ satisfy $\text{div}_h\,\mathbf{u} = f$, $\text{grad}_h\,\phi = \mathbf{u}$, in which the normal components of $\mathbf{u}$ arising in $\text{div}_h\,\mathbf{u}$ are to be evaluated in terms of the components given by $\text{grad}_h\,\phi$.

b. Across each oriented face $\delta\mathbf{S}$ impose the continuity conditions $[\mathbf{u} \cdot \delta S] = [\phi] = [\zeta] = 0$.

c. If $\delta S$ lies on the boundary $S$ of $V$, then $\phi$ and $\zeta$ are to be prescribed by the data.

These conditions exactly mirror the situation discussed for the one-dimensional problem. However, we shall find that they lead to an underdetermined system of algebraic equations and certain additional conditions will be required. These are furnished by the completeness conditions:

d. *Completeness Conditions*: These conditions determine $\zeta$ at vertex points in terms of the variable $\psi$ by the use of a bilinear interpolation which we indicate as $\zeta = \Omega(\psi)$. Among other things, this will ensure that is $\zeta$ bounded in norm by $\psi$.

This scheme will lead to an energy equation and convergence will be assumed. The potential form will also show that the maximum–minimum property also holds.

When curvilinear coordinates are used, many of the geometrical constructions required for elements will be provided analytically. Furthermore, for Cartesian or more general orthogonal grids, we will find that the variable $\zeta$ can be obtained by postprocessing the results using the completeness conditions. This emphasizes the practical advantages of utilizing

regular elements throughout most of the domain $V$ and restricting the general construction to boundary elements.

## 3.2. Geometrical Considerations and Notations

### *3.2.1. Normal Volume Elements*

We call $\{\delta V\}$ a *normal* covering of $V$ by volume elements $\delta V$, themselves called normal, if (i) each element is a hexahedron, some of whose face areas may be allowed to vanish providing its volume $\tau$ remains positive (*degeneracy*), (ii) any face of a boundary element $\delta V$ that is in contact with the boundary surface $S$ of $V$ is tangent to $S$ at the center point of the face. The first assumption has important consequences for the geometrical constructions, which will now be described.

Figure 2 indicates a normal volume $\delta V$ element with center at $P$ and surface elements $\delta \mathbf{S}$. Since $\delta V$ is a hexahedron, $P$ may be found as the average of the vertices of $\delta V$, while the average of the vertices on a face yields the center point $Q$ and the average of the vertex points on an edge yields the center point $R$. We may thus construct a right-handed, local coordinate basis

$$[\mathbf{e}(P)] \equiv (\mathbf{e}_1(P), \mathbf{e}_2(P), \mathbf{e}_3(P))$$

at $P$ which is formed by *unit* vectors in directions which connect the pairs of opposite center points of the faces $\delta \mathbf{S}$ which we denote as $Q_{i\pm}$, $i = 1, 2, 3$. The face $\delta \mathbf{S}(Q_{i-})$ is assumed oriented into $\delta V$, while $\delta \mathbf{S}(Q_{i+})$ is outward; these are sometimes called *inflow* and *outflow* faces. We also assume that the orientation carries over to neighboring elements by requiring that an outflow face from one element be an inflow face on its adjacent neighbor.

Our primary requirement will be to evaluate the vector $\mathbf{u}(Q)$ at the center points of faces. In order to do this we will construct a unit basis $[\mathbf{e}(Q)]$ at each $Q$ as follows: assume that $\delta \mathbf{S}(Q)$ is the outflow face of $\delta V(P)$ and the inflow face of a neighboring element $\delta V(P')$, e.g., $Q = Q_{1-}$. We take $\mathbf{e}_1(Q)$ as a unit vector in the direction of a line connecting $P$ and $P'$. Also take $\mathbf{e}_2(Q)$, $\mathbf{e}_3(Q)$ as unit vectors in directions that connect $Q$ with the center points of the edges $R$ of $\delta \mathbf{S}(Q)$ so that $[\mathbf{e}(Q)]$ forms a right-handed basis as indicated in the Fig. 2. Thus, $\mathbf{e}_2(Q)$, $\mathbf{e}_3(Q)$ are tangent vectors on $\delta \mathbf{S}(Q)$ while $\mathbf{e}_1(Q)$ is nontangential.

We may regard the points indicated as being related by displacement operators $E_{i\pm}$ along a direction $\mathbf{e}_i$ so that

$$Q_{i\pm} = E_{i\pm} P, \qquad R_{i\pm,j\pm} = E_{j\pm} Q_{i\pm}.$$

with the further understanding that $(i, j, k)$ indicates an even permutation of $(1, 2, 3)$. The averaging and difference operators defined earlier by (2.3) may be generalized by writing

$$\mu_i\phi(C) \equiv [\phi(E_{i+}, C) + \phi(E_{i-}, C)]/2, \qquad \Delta_i\phi(C) \equiv [\phi(E_{i+}, C) - \phi(E_{i-}, C)] \tag{3.1}$$

for a representative center point $C$. From this it is apparent that the summation-by-parts identities (2.4) continue to hold.

Motivated by this notation we will also $\Delta_i x(Q)$ to indicate the distance between the points $Q_{i-}$ and $Q_{i+}$ and write $h_i(Q) = \Delta_i x(Q)/2$. Also, $h$ itself will indicate the minimum value of $h_i(P)$ for all volume elements covering $V$.

### 3.2.2. *Covariant and Contravariant Bases on $\delta V$*

A basis $[\mathbf{e}] \equiv (\mathbf{e}_1, \mathbf{e}_2, \mathbf{e}_3)$ may be considered as a *covariant* basis from which a reciprocal *contravariant* basis $[\mathbf{e}]^{-1} \equiv (\mathbf{e}^1, \mathbf{e}^2, \mathbf{e}^3)$ can be constructed satisfying

$$\mathbf{e}^i = (\mathbf{e}_j \times \mathbf{e}_k)/\sqrt{e}, \qquad \mathbf{e}_i = \sqrt{\mathbf{e}} \cdot (\mathbf{e}^j \times \mathbf{e}^k), \qquad \mathbf{e}^i \cdot \mathbf{e}_j = \delta_{ij} \tag{3.2}$$

in which, if $\mathbf{e}_{ij} \equiv \mathbf{e}_i \cdot \mathbf{e}_j$ and $\mathbf{e}^{ij} \equiv \mathbf{e}^i \cdot \mathbf{e}^j$, then

$$\mathbf{e} \equiv \det(\mathbf{e}_{ij}), \qquad 1/\mathbf{e} = \det(\mathbf{e}^{ij}) \tag{3.3}$$

Anticipating the connection to curvilinear coordinates, we call $e_{ij}$ *element metric coefficients* at $P$. As a result we may write

$$\begin{gathered} \mathbf{u} = \sum u_i \mathbf{e}^i = \sum u^i \mathbf{e}_i \\ \mathbf{u}^i = \sum \mathbf{e}^{ij} u_j, \qquad u_i = \sum \mathbf{e}_{ij} \mathbf{u}^j \\ \mathbf{u} \cdot \mathbf{u} = \sum u_i u^i \end{gathered} \tag{3.4}$$

where $u_i = \mathbf{u} \cdot \mathbf{e}_i$ and $u^i = \mathbf{u} \cdot \mathbf{e}^i$ are the (physical) *covariant* and *contravariant* components of $\mathbf{u}$, respectively, with respect to $[\mathbf{e}]$.

Using the unit tangent vectors $\mathbf{e}_2, \mathbf{e}_3$ the oriented area of a face $\delta\mathbf{S}(Q_{1+})$ is

$$\delta\mathbf{S} = |\delta\mathbf{S}| \cdot \mathbf{e}_2 \times \mathbf{e}_3 = |\delta\mathbf{S}| \sqrt{\mathbf{e}} \cdot \mathbf{e}^1 \tag{3.5}$$

where

$$|\delta\mathbf{S}| = \Delta_2 x(Q)\, \Delta_3 x(Q)$$

Thus, the covariant component $\delta S_i$ of $\delta \mathbf{S}$ is $\delta S_i = |\delta \mathbf{S}| \sqrt{e}$. Also, elementary geometrical arguments based on the fact that normal volume elements are hexahedra show that if

$$\tau_0 = \Delta_1 x \cdot \Delta_2 x \cdot \Delta_3 x$$

then the volume measure $\tau$ of $\delta V$ is given by

$$\tau = \Delta_i x(Q)\, \mathbf{e}_i(P) \cdot [\delta \mathbf{S}(Q_{i\ -}) + \delta \mathbf{S}(Q_{i,+})]\, 2 = \tau_0 \cdot \mu_i \sqrt{e}$$

$i = 1, 2, 3$. If we also assume positive constants $c_0$ and $c_1$ such that $c_0 h^3 \leqslant \tau \leqslant c_1 h^3$ and also set $\sqrt{e_0} \equiv \mu_i \sqrt{e}$ we can summarize these geometrical results as

$$\tau = \tau_0 \cdot \sqrt{e_0}, \qquad \delta S_i = \Delta_j x \, \Delta_k x \, \sqrt{e} \tag{3.6}$$

Finally, we also observe that midpoint quadrature rules result in

$$\int \mathbf{u} \cdot d\mathbf{x} \approx \mathbf{u}(C) \cdot \Delta \mathbf{x}(C)$$

$$\int \mathbf{u} \cdot d\mathbf{S} \approx \mathbf{u}(C) \cdot \delta \mathbf{S}(C) \tag{3.7}$$

$$\int \mathbf{u} \cdot dV \approx \mathbf{u}(C) \cdot \tau$$

where $C$ is a representative center point of the figure.

These facts summarize the principal properties of normal volume elements that we shall require.

### 3.3. The Operators $\mathrm{div}_h$ and $\mathrm{grad}_h$

The fundamental geometrical properties of the differential operators div, curl, and grad stem from the following: div relates volume integrals with surface integrals, curl relates surface integrals with line integrals, and grad relates line integrals with endpoints. We will now describe how these properties can be systematically developed for the div and grad operators.

*$div_h$*: Gauss' formula

$$\int \mathrm{div}\, \mathbf{u}\, dV = \int \mathbf{u} \cdot \mathbf{n}\, dS$$

when applied on $\delta V$ using the quadrature approximations indicated above suggests the definition

$$\tau\, \mathrm{div}_h\, \mathbf{u} \equiv \sum_i \Delta_i \mathbf{u} \cdot \delta \mathbf{S} \tag{3.8}$$

in which the difference operator applies to opposite face center points $Q_{i\pm}$. Using the component representations for the terms on the right,

$$\mathrm{div}_h\,\mathbf{u} = \tau^{-1}\sum_i \Delta_i u^i \cdot \delta S_i \tag{3.9}$$

or, noting (3.6),

$$\mathrm{div}_h\,\mathbf{u} \equiv (\sqrt{e_0})^{-1}\sum_i \Delta_i \sqrt{e}\, u^i/\Delta_i x \tag{3.10}$$

*grad*$_h$: The approximations to be identified with $\mathbf{u} = \mathrm{grad}\,\phi$ will follow from the line-integral evaluation

$$\int_C \mathbf{u}\cdot d\mathbf{x} = \phi(B) - \phi(A) \tag{3.11}$$

in which $A, B$ are end points of a curve $C$. We will describe how the covariant components of $\mathbf{u}$ with respect to the bases $[\mathbf{e}(Q)]$ can be determined at face center points.

*Tangential Components.* Recalling earlier notations, suppose $\mathbf{e}_2(Q_{1+})$, $\mathbf{e}_3(Q_{1+})$ are tangent vectors to the face $\delta\mathbf{S}(Q_{1+})$ at $Q_{1+}$. Evaluating (3.11) along the line connecting the centers of opposite edges $R_{1+,2\pm}$ and $R_{1+,3\pm}$ we obtain

$$\int_C \mathbf{u}\cdot d\mathbf{x} = \zeta(R_{1+,j+}) - \zeta(R_{1+,j-}), \qquad j = 2, 3$$

in which we have identified the potential variable on edges of $\delta\mathbf{S}$ by $\zeta$. Next, use the quadrature evaluation

$$\int_C \mathbf{u}\cdot d\mathbf{x} = \Delta_j x\cdot[\mathbf{u}\cdot\mathbf{e}_j(Q_{1+})] = \Delta_j x\cdot u_j(Q_{1+})$$

in which $u_j$ is the covariant component of $\mathbf{u}(Q_{1+})$. Thus,

$$\begin{aligned}\Delta_j x\cdot u_j(Q_{1+}) &= \zeta(R_{1+,j+}) - \zeta(R_{1+,j-}), \qquad j = 2, 3\\ &\equiv \Delta_j\zeta(Q_{1+})\end{aligned} \tag{3.12}$$

*Nontangential Components.* We will also require evaluations of the non-tangential components of $\mathbf{u}$ at the center points of faces and, as for the one-dimensional case, want to evaluate these in terms of the value of $\psi$ at the center $P$ of $\delta V$ and of $\phi$ at the center points $Q$ of its faces. Let us first introduce the one-sided difference operators

$$\Delta_i^{\pm}\phi(Q_{i\pm}) \equiv \pm[\phi(Q_{i\pm}) - \psi(P)] \tag{3.13}$$

Then (3.8) leads to

$$\int \mathbf{u} \cdot d\mathbf{x} = \Delta_i^{\pm} \phi(Q_{i\pm})$$

in which the line integrals are to be taken between $Q_i$ and $P$ and between $P$ and $Q_{i+}$, respectively. We then evaluate the integrals by *one-sided* quadrature approximations using values of $\mathbf{u}$ at the faces to obtain

$$\int \mathbf{u} \cdot d\mathbf{x} \approx (\Delta_i x(P)/2) \cdot \mathbf{u}(Q_{i\pm}) \cdot \mathbf{e}_i(Q_{i\pm})$$

$$= (\Delta_i x(P)/2) \cdot u_i(Q_{i\pm})$$

so that

$$[\Delta_i x(P)/2] \cdot u_i(Q_{i\pm}) = \Delta_i^{\pm} \phi(Q_{i\pm}) = \pm[\phi(Q_{i\pm}) - \psi(P)] \tag{3.14}$$

We can *summarize* this construction as follows: $\text{grad}_h$: $u(Q) = \text{grad}_h \phi$ expresses the set of relationships between the covariant components of $u(Q)$ and values of $\phi$, $\psi$, and $\zeta$ at points $Q$ on the faces of an element given by:

*Tangential Components*:

$$\Delta_j x \cdot u_j(Q) = \Delta_j \zeta(Q) \tag{3.12}$$

*Nontangential Components*:

$$(\Delta_i x/2)\, u_i(Q) = \Delta_i^{\pm} \phi(Q) \tag{3.14}$$

where

$$\Delta_i^{\pm} \phi(Q) \equiv \pm[\phi(Q) - \psi(P)] \tag{3.13}$$

Equations (3.14) should be compared to Eqs. (2.6). By adding and subtracting these terms we obtain an equivalent form:

$$\begin{aligned} \Delta_i x(P)\, \mu_i u_i(P) &= \Delta_i \phi(P) \\ \psi(P) &= \mu_i \phi(P) - \Delta_i x(P)\, \Delta_i u_i(P)/4 \end{aligned} \tag{3.15}$$

in which only centered operators at $P$ are involved and which may be seen to be second-order accurate with respect to $P$. These forms play an important role in establishing energy results.

### 3.4. A Compact Scheme

We will now return to the primary problem of solving the boundary value problem when $V$ is a general volume with boundary $S$. Following our

earlier discussion, we describe a compact scheme for solving the problem as follows:

(i) In each element $\delta V$ solve

$$\operatorname{div}_h \mathbf{u} = f, \qquad \mathbf{u} = \operatorname{grad}_h \phi \tag{3.16}$$

Note that $\operatorname{div}_h \mathbf{u} = f$ provides one equation for the six contravariant components of $\mathbf{u}$ on the faces of the element, while $\mathbf{u} = \operatorname{grad}_h \phi$ expresses three equations for the covariant components of $\mathbf{u}$ on each of the six sides of $\delta V$, in which the tangential components are evaluated in terms of the variable $\zeta$ at the center points of edges while the nontangential components are determined by the variables $\phi$ and $\psi$.

(ii) Use

$$u^i = \sum e^{ij} u_j \tag{3.17}$$

from (3.4) to relate the contravariant components to the covariant components arising in (3.16).

An important simplification will occur in this construction whenever $e^{ij} = 0$, $i \neq j$. When this situation arises we call the scheme *strongly* compact; otherwise we use the term *weakly* compact. For a strongly compact scheme the tangential components of $\mathbf{u}$ on faces will not affect the computation directly (and, thus, neither will the variable $\zeta$) but may, if required, be determined in terms of the variable $\zeta$ by a postprocessing technique using the completeness relationships described below. This arises when Cartesian or orthogonal curvilinear grids are involved.

(iii) Impose *continuity conditions* for $\mathbf{u}$, $\phi$, $\zeta$ on faces common to neighboring elements. In case $\delta V$ is a boundary element, the data on $S$ will be assumed to determine the data $\phi$ and $\zeta$ on any face tangent to $S$ by the use of a Taylor series approximation.

We are required to calculate $\mathbf{u}$ and $\phi$ at the centers of the faces of elements, $\psi$ at the centers of the elements themselves, and $\zeta$ on the edges of the faces. By examining a cube, we can verify the fact that the number of unknowns involved in the system of equations resulting from the steps just described will exceed the number of equations by just the number of interior edges of elements, i.e., those edges that are incident to four adjacent elements. This same result will also hold for a more general covering $\{\delta V\}$. In order to make the scheme determinate we will add the following completeness conditions.

(iv) *Completeness Conditions*: Let $N(R)$ denote the center points $P$ of those volume elements that are incident to an edge having $R$ as center

point. Using a bilinear interpolation, express $\zeta(R)$ in terms of the values $\psi(R)$ which are associated with the neighboring elements. The result can be written

$$\zeta(R) = \sum \omega(P)\,\psi(P) \tag{3.18}$$

where the summation includes points $P$ in $N(R)$ and the weights $\omega$ are non-negative and sum to 1. As noted above, when the scheme is strongly compact (3.18) will allow the tangential components of $\mathbf{u}$ on faces to be calculated separately.

### 3.5. Energy

We will now show how an energy expression can be derived. From it the existence and uniqueness of the solution of the discrete problem will follow.

Following the argument given for the one-dimensional case, use the summation rules (2.9) and also (3.18) to obtain

$$\begin{aligned}
\tau \operatorname{div}_h \phi \mathbf{u} &= \sum_i \Delta_i \phi u^i\, \delta S_i \\
&= \sum_i \left[\mu_i \phi\, \Delta_i u^i\, \delta S_i + \Delta_i \phi \mu_i u^i\, \delta S_i\right] \\
&= \sum_i \left[\left(\psi + \tfrac{1}{4}\Delta_i x\, \Delta_i u_i\right) \Delta_i u^i\, \delta S_i + \Delta_i x \mu_i u_i (\mu_i u^i\, \delta S_i)\right] \\
&= \psi \sum_i \Delta_i u^i\, \delta S_i + \sum_i \Delta_i x \mu_i (u_i u^i\, \delta S_i)
\end{aligned}$$

or, recalling that $\delta S_i = \sqrt{e}\,\Delta_j x\, \Delta_k x$,

$$\tau \operatorname{div}_h \phi \mathbf{u} = \phi \tau \operatorname{div}_h \mathbf{u} + \tau_0 \sum_i \mu_i (u_i u^i \sqrt{e})$$

so that summing over volume elements yields

$$\sum_V \operatorname{div}_h \phi \mathbf{u} \tau = \sum_V \phi \operatorname{div}_h \mathbf{u} \tau + \sum_V \left\{ \sum_i \mu_i (u_i u^i \sqrt{e}) \right\} \tau_0$$

Finally, using the telescoping property of the $\sum_V \operatorname{div}_h$ term on the left-hand side and recalling that $\tau = \tau_0 \sqrt{e_0}$, we find

$$\sum_S \phi \mathbf{u} \cdot \delta \mathbf{S} = \sum_V \phi \operatorname{div}_h \mathbf{u} \tau + \sum_V \mathbf{u} \cdot \mathbf{u} \tau \tag{3.19}$$

which is clearly consistent with the integral form of the energy equation given by Eq. (1.4). Noting that (3.19) will ensure that $\zeta$ is bounded in norm by $\psi$, the same arguments as were given for the one-dimensional problem will imply that *this more general compact scheme converges and yields second-order accuracy for* $\phi$, $\psi$, $\zeta$ *and* $\mathbf{u}$.

### 3.6. The Potential Formulation

We shall indicate how the scheme just described can be formulated solely in terms of $\phi$, $\psi$, and $\zeta$, corresponding to the potential form $\nabla^2\phi = f$. Again following our discussion of the one-dimensional case, we write, using (3.9) and (3.4),

$$\tau \operatorname{div}_h \mathbf{u} = \sum_i \Delta_i u^i \, \delta S_i$$

$$= \sum_i \Delta_i \left( \sum_j e^{ij} u_j \right) \delta S_i$$

or, regrouping terms:

$$\tau \operatorname{div}_h \mathbf{u} = \sum_i \Delta_i e^{ii} u_i \, \delta S_i + \sum_i \left( \Delta_i \sum_{j \neq i} e^{ij} u_j \right) \delta S_i \tag{3.20}$$

Using (3.14) in the first summation we find

$$\sum_i \Delta_i e^{ii} u_i \, \delta S_i = 2 \sum_i \Delta_i e^{ii} \, \Delta_i^{\pm} \phi \, \delta S_i / \Delta_i x$$

$$= 4 \sum_i \mu_i e^{ii} \phi \, \delta S_i / \Delta_i x - 4\psi(P) \sum_i \mu_i e^{ii} \, \delta S_i / \Delta_i x \tag{3.21}$$

in which the summands are evaluated at the centers of faces about the center point $P$ of the element. The second group of terms in (3.20) involve only tangential components of $\mathbf{u}$ at face centers, and we may use (3.12) to express these in terms of values of $\zeta$ at the edges. In this manner, all of the terms in (3.20) may be expressed in terms of the values of $\phi$, $\psi$, and $\zeta$ in each element. This leads to the *potential* operator $\operatorname{div}_h \operatorname{grad}_h \phi$.

Since $\phi$, $\psi$, and $\zeta$ are assumed continuous across faces, the continuity conditions for $\mathbf{u}$ across a face $\delta S_i$ common to neighboring elements with centers at $P$ and $P'$ reduce to

$$[u^i \, \delta S_i] = 0$$

The tangential covariant components of $\mathbf{u}$ are continuous, since they are

determined by $\zeta$. Recalling (3.14), the condition that the nontangential covariant component $u_i$ be continuous is then

$$(\Delta_i x + \Delta_i x')\phi = \Delta_i x\psi' + \Delta_i x'\psi \tag{3.22}$$

which may be compared to (2.9a).

Consider the treatment of $\nabla^2\phi = 0$ using a strongly compact scheme. In this case $e^{ij} = 0$, $j \neq i$ and the condition $\operatorname{div}_h \operatorname{grad}_h \phi = 0$ as expressed by using (3.20) reduces to

$$\sum_i \mu_i e^{ii}\phi\, \delta S_i/\Delta_i x = \psi(P) \sum_i \mu_i e^{ii}\, \delta S_i/\Delta_i x \tag{3.23}$$

which may be written

$$\psi = \sum_i \alpha_i \phi \tag{3.24}$$

where

$$\alpha_i = (\mu_i e^{ii}\, \delta S_i/\Delta_i x) \Big/ \left( \sum_i \mu_i e^{ii}\, \delta S_i/\Delta_i x \right)$$
$$\sum_i \alpha_i = 1 \tag{3.25}$$

If we write the continuity condition (3.22) as

$$\phi = \beta_i \psi + \beta_i' \psi', \qquad \beta_i + \beta_i' = 1 \tag{3.26}$$

we can conclude that the maximum–minimum property holds. This same conclusion can be reached for a weakly compact scheme.

Referring to the energy expression, it will be seen that the potential form can also be viewed as arising from a variational problem. By using the completeness relations, the computational problem will thus reduce to determining the variables $\phi$ and $\psi$ associated with a symmetric, positive definite matrix and thereby allows a variety of familiar solution techniques to be used.

### 3.7. Degeneracy

Recall that the definition of a normal volume element allowed for the area of one or more of its faces to vanish. Such degenerate elements play a natural role at the boundary $S$ and are especially relevant, as will be shown shortly, in treating problems in curvilinear coordinate at the origin.

Let us suppose that a face with center $Q$ is degenerate, i.e., $d\mathbf{S}(Q) = 0$. Referring to (3.8) we see that the term involving the factor $d\mathbf{S}(Q)$ will not contribute to the evaluation of $\mathrm{div}_h \mathbf{u}$ and, as a result, the contravariant component of $\mathbf{u}(Q)$ need not be computed on the face. In the potential form, this simply modifies the weight $\alpha$ associated with the degenerate face in (3.25).

## 3.8. Curvilinear Coordinates

We will illustrate how the discussion applies when curvilinear coordinates are used. With their use the basis $(\mathbf{e}_i, \mathbf{e}_j, \mathbf{e}_k)$, which was required at each face of a volume element, can be constructed analytically, thereby considerably reducing the preliminary computational steps required. Using the potential form, we shall also illustrate the treatment of the situation at the origin that gives rise to degeneracy.

We indicate by $\mathbf{x} = \mathbf{x}(\mathbf{q})$ a mapping in general curvilinear coordinates. The vectors

$$\mathbf{g}_i = \frac{\partial \mathbf{x}}{\partial \mathbf{q}^i} \tag{3.27}$$

are tangent vectors on the coordinate lines formed by $q^j = \text{const}$ and $q^k = \text{const}$ so that an element of length is determined by

$$ds^2 = \sum\sum g_{ij}\, dq^i\, dq^j$$

in which $g_{ij}$ are metric coefficients given by $g_{ij} = \mathbf{g}_i \cdot \mathbf{g}_j$. Considering $[\mathbf{g}] = (\mathbf{g}_i, \mathbf{g}_j, \mathbf{g}_k)$ as a covariant basis, a reciprocal basis $(\mathbf{g}^i, \mathbf{g}^j, \mathbf{g}^k)$ is given as

$$\mathbf{g}^i = (\mathbf{g}_j \times \mathbf{g}_k)/\sqrt{g}$$

in which $\mathbf{g} = \det(g_{ij})$. Also, if $g^{ij} \equiv \mathbf{g}^i \cdot \mathbf{g}^j$, then $\det(g^{ij}) = g^{-1}$.

Consider a curvilinear volume element $dV$ which is formed as the image of a rectilinear volume element whose volume is $dq^i\, dq^j\, dq^k$. Then the edges of a face on $dV$ given as $q^i = \text{const}$ are coordinate lines on which $\mathbf{g}_j, \mathbf{g}_k$ are tangent vectors and the oriented area of the face is

$$d\mathbf{S} = (\mathbf{g}_j \times \mathbf{g}_k)\, dq^j\, dq^k$$

We may associate a normal volume element $\delta V$ with $dV$ by constructing tangent planes through the centers of the surface elements through $dV$. From geometrical considerations it is evident that if we make the following identifications

$$A_i \times \mathbf{e}_i = \mathbf{g}_i\, dq^i, \qquad i = 1, 2, 3 \tag{3.28}$$

the results of our earlier discussion will apply. If $u^i(\mathbf{g})$ indicates a contravariant component of $\mathbf{u}$ in the curvilinear system we find, in place of (3.10),

$$\operatorname{div}_h \mathbf{u} \equiv (\sqrt{g_0})^{-1} \sum_i \Delta_i \sqrt{\mathbf{g}}\, u^i(\mathbf{g})/dq^i \tag{3.29}$$

Similarly, $\mathbf{u} = \operatorname{grad}_h \phi$, expressed earlier by (3.12) and (3.14), now result in the following components.

*Tangential Components*:

$$dq^j \cdot u_j(\mathbf{g}) = \Delta_j \zeta \tag{3.30}$$

*Nontangential Components*:

$$(dq^i/2)\, u_i(\mathbf{g}) = \Delta_i^{\pm} \phi \tag{3.31}$$

*Examples*

The cases of cylindrical and spherical coordinates may help illustrate these results.

*Cylindrical Coordinates.* Here $\mathbf{q} = (r, \theta, z)$ and a calculation gives $\sqrt{g} = r$ and $\sqrt{g}\, g^{11} = r$, $\sqrt{g}\, g^{22} = 1/r$, $\sqrt{g}\, g^{33} = r$. The center points of faces $Q_{i\pm}$ have the coordinates

$$P_{1\pm} = (r \pm \Delta r/2, \theta, z), \qquad P_{2\pm} = (r, \theta \pm \Delta\theta/2, z), \qquad P_{3\pm} = (r, \theta, z \pm \Delta z/2)$$

Adopting more standard finite difference notations, let $\phi(i\,\Delta r, j\,\Delta\theta, k\,\Delta z) \equiv \phi_{i,j,k}$ and extend the meaning of the spatial averaging and differencing operators $\mu$, $\Delta$ to this case by writing $(\mu_r, \mu_\theta, \mu_z)$, $(\Delta_r, \Delta_\theta, \Delta_z)$. We find that in a cell with center at $P = (i\,\Delta r, j\,\Delta\theta, k\,\Delta z)$

$$\operatorname{div}_h \operatorname{grad}_h \phi = \frac{4}{r}\left\{\frac{1}{2\,\Delta r^2}\left[(r + \Delta r/2)\,\phi_{i+1/2,j,k} + (r - \Delta r/2)\right]\phi_{i-1/2,j,k}\right.$$

$$\left. + \frac{1}{r\,\Delta\theta^2}\mu_\theta \phi_{i,j,k} + \frac{r}{\Delta z^2}\mu_z \phi_{i,j,k} - \sigma_0 \psi_{i,j,k}\right\} \tag{3.32}$$

in which

$$\sigma_0 = r\left(\frac{1}{\Delta r^2} + \frac{1}{\Delta z^2}\right) + \frac{1}{r\,\Delta\theta^2}$$

Assuming equal spacings, the continuity conditions across faces have the form

$$\phi = \mu\psi \tag{3.33}$$

in which $\mu = (\mu_r, \mu_\theta, \mu_z)$.

A cell with center at $(\Delta r/2, j\,\Delta\theta, k\,\Delta z)$ has the origin as a degenerate face. In this case we see that the coefficient of the value of the unknown $\phi_{0,j,k}$ vanishes, so that *no assumption other than boundedness* at the origin is required for the scheme.

For cells not involving boundary points, we may use the continuity condition in (3.29) to express the result solely in terms of $\psi$. By adopting the notation $\delta_r \equiv \Delta_r/\Delta r$, etc. to indicate divided differences, the potential operator for such cells reduces to the form

$$\operatorname{div}_h \operatorname{grad}_h \phi = \left\{ \delta_r^2 + \frac{1}{r}\,\delta_r \mu_r + \frac{1}{r^2}\,\delta_\theta^2 + \delta_z^2 \right\} \psi \tag{3.34}$$

which can be seen to be consistent with the familiar differential form in cylindrical coordinates. However, we emphasize again that the boundary conditions involving $\phi$ cannot be handled directly from this form but must, instead, be developed using (3.30) directly.

*Spherical Coordinates.* In this case $\mathbf{q} = (r, \varphi, \theta)$ and a calculation shows $\sqrt{g} = r^2 \sin\varphi$ while $\sqrt{g}\,g^{11} = r^2$, $\sqrt{g}\,g^{22} = \sin\varphi$, $\sqrt{g}\,g^{33} = 1$. Again assuming a uniform mesh spacing, we find in

$$\begin{aligned} \operatorname{div}_h \operatorname{grad}_h \phi = \frac{4}{r^2 \sin\chi} \Bigg\{ & \frac{\sin\chi}{2\,\Delta r^2} \left[ (r + \Delta r/2)^2\, \phi_{i+1/2,j,k} + (r - \Delta r/2)^2\, \phi_{i-1/2,j,k} \right] \\ & + \frac{1}{2r\,\Delta\chi^2} \left[ \sin(\chi + \Delta\chi/2)\, \phi_{i,j+1/2,k} + \sin(\chi - \Delta\chi/2)\, \phi_{i,j-1/2,k} \right] \\ & \times \frac{1}{\Delta\theta^2}\, \mu_\theta \phi_{i,j,k} - \sigma_0 \psi_{i,j,k} \Bigg\} \end{aligned} \tag{3.35}$$

in which

$$\sigma_0 = \left\{ \frac{1}{\Delta r^2} (r^2 + \Delta r^2/2) \sin\chi + \frac{1}{\Delta\chi^2} (\sin\chi \cos \Delta\chi/2) + \frac{1}{\Delta\theta^2} \right\}$$

With $\mu = (\mu_r, \mu_\chi, \mu_\theta)$ the continuity conditions again lead to $\phi = \mu\psi$. We see that the situation at the origin is exactly similar to that in the previous example; in particular, only the boundedness of the solution at the origin is required. Away from boundary cells, the continuity conditions can be used to reduce matters to the form

$$\begin{aligned} \Delta_t \psi = \frac{\Delta t}{r^2 \sin\chi} \Big\{ & (r^2 + \Delta r^2/2) \sin\chi\, \delta_r^2 + 2 \sin\chi\, \delta_r \mu_r \\ & + (\sin\chi \cos \Delta\chi/2)\, \delta_\chi^2 + \delta_\theta^2 \Big\} \psi \end{aligned} \tag{3.36}$$

which can be seen to be consistent with the potential form of the diffusion equation in spherical coordinates. We again add a precautionary note about attempting to treat the boundary conditions involving $\phi$ from this form.

### 3.9. The $\text{curl}_h$ Operator

In our treatment of $\mathbf{u} = \text{grad}_h \phi$, emphasis was placed on evaluating the tangential components of $\mathbf{u}$ at the center $Q$ of each face $\delta\mathbf{S}$ using a covariant basis $[\mathbf{e}(Q)]$. Using (3.12), these were expressed in terms of the variable $\zeta$ which was associated with the center points of the edges of the face. The completeness conditions (3.18) were then used to relate $\zeta$ to $\psi$. The contravariant component of $\mathbf{u}$ which arose in the definition of $\text{div}_h \mathbf{u}$ were evaluated in terms of these covariant components using (3.4).

It is desirable, also, to also have a finite volume approximation to the curl operator, which we will indicate by $\text{curl}_h \mathbf{u}$. A satisfactory calculus would then yield both $\text{div}_h \text{curl}_h \mathbf{u} = 0$ as well as $\text{curl}_h \text{grad}_h \phi = 0$ as identities. We shall now indicate how this may be accomplished.

In Fig. 2, $T$ indicated a representative vertex of an element. Let $[\hat{\mathbf{e}}(T)]$ indicate a basis formed by the edges which intersect at $T$ using the orientation established by $[\mathbf{e}(P)]$; also let $\hat{\mathbf{e}}(R)$ indicate the translation of $\hat{\mathbf{e}}(T)$ to the center point $R$ of an edge $TT'$. A suitable definition of $\text{curl}_h$ is suggested by the following: If $\omega = \text{curl}\, \mathbf{u}$, then a quadrature approximation in Stokes' formula

$$\int_{\delta S} \omega \cdot d\mathbf{S} = \int_{\partial \delta S} \mathbf{u} \cdot d\mathbf{s}$$

leads to

$$\omega \cdot \delta S \approx \Delta_k x \cdot \Delta_j (\mathbf{u} \cdot \hat{\mathbf{e}}_k) - \Delta_j x \cdot \Delta_k (\mathbf{u} \cdot \hat{\mathbf{e}}_j)$$

involving the edges of a face $\delta\mathbf{S}$. Using component representations, we are led to define $\text{curl}_h$ in terms of the *set of contravariant components* $\omega^i$ *associated with the faces of* $\delta V$ by means of

$$\omega = \text{curl}_h \mathbf{u} \Rightarrow \omega^i \equiv (\Delta_j \hat{u}_k / \Delta_j x - \Delta_k \hat{u}_j / \Delta_k x) \tag{3.37}$$

in which the covariant components $\hat{u} = \mathbf{u} \cdot \hat{\mathbf{e}}$. With this definition the identity

$$\text{div}_h \text{curl}_h \mathbf{u} = 0 \tag{3.38}$$

follows by noting the cancellation of "line integrals" along the common edge of faces. [It is also possible to identify a vector associated with the

center point of $dV$, say $\langle \text{curl}_h \mathbf{u} \rangle \equiv \sum \mu_i \omega^i \mathbf{e}_i(P)$, but this vector will not be annihilated by $\text{div}_h$ and for that reason will not be considered further here.]

As already noted, our earlier treatment of $\mathbf{u} = \text{grad}_h \phi$ will not furnish a direct means of evaluating the covariant components $\hat{u}$ occurring above and thus we cannot interpret $\text{curl}_h \text{grad}_h \phi$. In order to overcome this, introduce a new variable $\chi$ which will be defined at vertices $T$ and is often called a *box-variable*. Recalling the intrinsic definition of grad indicated by (3.11), we will define $\text{grad}_h$ along edges by

$$\Delta_i x \cdot \hat{u}_i(R) = \Delta_i \chi(R) \tag{3.39}$$

in which $\Delta_i x$ is the distance between vertices along an edge with direction $\hat{\mathbf{e}}_i$ on which $R$ is the center point and $\Delta_i \chi(R)$ is the difference in values of $\chi$ at the vertex neighbors of $R$. Then

$$\omega^i(\hat{\mathbf{u}}) \equiv (\Delta_j \Delta_k \chi - \Delta_k \Delta_j \chi) \div \Delta_j x \cdot \Delta_k x \equiv 0$$

i.e.,

$$\text{curl}_h \text{grad}_h \phi \equiv 0 \tag{3.40}$$

This suggests a theoretical advantage in using the box-variable $\chi$ instead of $\zeta$ which was used in the earlier discussions. The most direct way to accomplish this is to define the edge variable $\zeta(R)$ as the average of $\chi$ at vertices neighboring $R$, i.e., $\zeta = \mu\chi$, and also reexpress the consistency conditions (3.18) so that now $\chi(T)$, rather than $\zeta(R)$, will be related to $\psi(P)$ at each interior vertex by a bilinear interpolation of the form $\chi = \Omega(\psi)$, which will now involve the six neighboring elements having $T$ as a vertex.

## 4. THE TIME-DEPENDENT PROBLEM

### 4.1. The Potential Form

The potential form of the time-dependent diffusion equation (1.1) is, with $f = 0$,

$$\phi_t = \text{div grad } \phi \tag{4.1}$$

The discrete finite volume operator $\text{div}_h \text{grad}_h \phi$ corresponding to $\text{div grad}\, \phi$ has been shown to yield a discrete energy expression which corresponds to the time-independent energy terms in (3.19). The principal question remaining, therefore, is how to include the term $\phi_t$ in the numerical scheme

which will provide the approximation to the term $(d/dt)\int \phi^2\, dV$ in the energy expression.

Divide $[0, T]$ into $N$ equal parts of width $\Delta t$, write $t_n = n\,\Delta t$, and adopt the standard finite difference notation $u(n\,\Delta t) = u^n$. Also, let $\mu_t$, $\Delta_t$ indicate the central averaging and difference operators which effect the time index as indicated:

$$\begin{aligned} \mu_t u^n &= (u^{n+1/2} + u^{n-1/2})/2 \\ \Delta_t u^n &= (u^{n+1/2} - u^{n-1/2}) \end{aligned} \tag{4.2}$$

From (2.4) it is evident that

$$\mu_t \psi^n\, \Delta_t \psi^n = \tfrac{1}{2}\Delta_t (\psi^n)^2 \tag{4.3}$$

We will consider the following *three-level* compact scheme.

*A. Compact Scheme.*

$$\Delta_t \psi^n = \Delta t\, \mathrm{div}_h \,\mathrm{grad}_h\, \phi^n \tag{4.4}$$

$$\psi^n = \mu_t \psi^n \tag{4.5}$$

to which the appropriate continuity and completeness conditions (3.22) and (3.18) are understood to apply. By multiplying (4.4) by $\psi^n$ we obtain

$$\tfrac{1}{2}\Delta_t (\psi^n)^2 = \Delta t \cdot \psi^n\, \mathrm{div}_h \,\mathrm{grad}_h\, \phi^n \tag{4.6}$$

in a volume element. The term on the right-hand side has already been shown to lead to the energy expression (3.19). Thus, by summing (4.6) over elements in a time-strip and using the implied continuity conditions across faces we will obtain

$$\sum_{\nu} \tfrac{1}{2}\Delta_t (\psi^n)^2\, \tau + \Delta t \sum_{\nu} \mathbf{u}^n \cdot \mathbf{u}^n \tau = \Delta t \sum_{S} \phi^n \mathbf{u}^n \cdot \delta \mathbf{S} \tag{4.7}$$

which is the discrete energy expression that was expected.

Assuming dissipative boundary conditions in the sense of Kreiss (1964), it is evident from this result that we can conclude: *both $\psi^n$ and $\phi^n$ are bounded in a discrete norm by the initial and boundary data. Because the scheme is consistent, this also implies that the scheme converges.* (Our previous discussion of the maximum–minimum property can allow us to conclude convergence as well.)

We can summarize this in several equivalent ways, in each of which the additional continuity and completeness conditions are assumed to apply:

*B. Two-Step.*

$$\psi^{n+1/2} - \psi^n = (\Delta t/2)\,\mathrm{div}_h\,\mathrm{grad}_h\,\phi^{n+1/2} \tag{4.8a}$$

and

$$\psi^{n+1} - \psi^{n+1/2} = (\Delta t/2)\,\mathrm{div}_h\,\mathrm{grad}_h\,\phi^{n+1/2} \tag{4.8b}$$

As above, this is a *two-step scheme* in which the first requires solving the equations in a time strip for $\phi^{n+1/2}$ and $\psi^{n+1/2}$ *implicitly* in terms of the boundary data for $\phi(t_{n+1/2})$ and the initial data $\psi^n$. With these values determined, then $\psi^{n+1}$ can be determined *explicitly* from the second set of equations and furnishes initial data for the next time strip.

*C. One-Step.*

Eliminating $\psi^n$ in the above scheme we find

$$\Delta_t \psi^n = \Delta t\,\mu_t\,\mathrm{div}_h\,\mathrm{grad}_h\,\phi^n \tag{4.9}$$

This is a *one-step Crank–Nicholson form.*

*Example.* Using our earlier one-dimensional notations, consider the treatment of $\phi_t = \phi_{xx}$. We find that the one-step scheme may be written in potential form as

$$\Delta_t \psi_i^n = \kappa\mu_t(\mu\phi_i^n - \psi_i^n), \qquad i \in I_c \text{ (center points)} \tag{4.10a}$$

where $\kappa = \Delta t/h^2$, $h = \Delta x/2$. To this we add the continuity conditions in the form

$$\mu\psi_i^{n+1/2} - \phi_i^{n+1/2} = 0, \qquad i \in I_e \text{ (end points)} \tag{4.10b}$$

Comparing with (2.9) we again recognize that the variables $\phi_i$, $\psi_i$ are the odd–even components of a tridiagonal system and are therefore readily obtained at each time step.

Numerical tests using the solution $\phi = \exp(t - x)$ with initial conditions at $t = 0$ produced the following (max) error norms for $\phi$ and $\phi_x$ at $t = 1$ in which $\Delta t = \Delta x$:

| Total number of points | $\phi$ error | $\phi_x$ error |
|---|---|---|
| 9 | 0.00116002 | 0.0186447 |
| 17 | 0.00029997 | 0.00485956 |
| 33 | 0.0000768122 | 0.00123751 |

These results appear to verify the accuracy asserted by the theory.

## 4.2. An ADI Scheme

Except for the one-dimensional example just considered, the basic scheme (4.4) is implicit and effective solution methods must be considered in order to treat the general problem in higher dimensions in a practical manner. It is especially desirable that a proposed method also provide an effective means of treating the steady-state problem as well. We will now show that a Peaceman–Rachford-type ADI scheme, using a straightforward treatment of intermediate boundary conditions, can solve the finite-volume problem with second-order accuracy in both space and time. Again, the existence of an energy estimate will provide the key to convergence.

We will find it convenient to make a few slight changes in some of our notations. First, we will let $\bar{v}$ indicate the time average of a variable $v$, i.e., let

$$\bar{v}^n \equiv \mu_t v^n \tag{4.11}$$

Also, we let

$$F_i^n \equiv \tau^{-1} \Delta_i (\mathbf{u}^n \cdot d\mathbf{S}_i) \tag{4.12}$$

so that (3.9) leads to

$$\operatorname{div}_h \mathbf{u}^n \equiv F_1^n + F_2^n + F_3^n$$

Then, for example, the one-step scheme (4.10) can be written as

$$\Delta_t \psi^n = \Delta t (\bar{F}_1^n + \bar{F}_2^n + \bar{F}_3^n) \tag{4.13}$$

in which $\mathbf{u} = \operatorname{grad}_h \phi$. Finally, we indicate by $g^n$ assumed boundary data for $\phi$ on $S$ at time $t^n$.

Limiting our discussion to two dimensions, consider the following two-step scheme:

$$\psi^{n+1/2} - \psi^n = (\Delta t/2)(F_1^{n+1/2} + F_2^n) \tag{4.14a}$$

$$\psi^{n+1} - \psi^{n+1/2} = (\Delta t/2)(F_1^{n+1/2} + F_2^{n+1}) \tag{4.14b}$$

and note its similarity to (4.8). Recalling our discussion of the one-dimensional example, it is evident that the first step can be solved as a one-dimensional problem using boundary conditions $\phi^{n+1/2} = g^{n+1/2}$. We solve the second step similarly, but with the boundary conditions $\phi^{n+1} = g^{n+1}$.

Adding and subtracting (4.14a) and (4.14b), and relabeling the time level for purposes of later discussion, we find

$$\psi^{n+1/2} - \psi^{n-1/2} = \Delta t (F_1^n + \bar{F}_2^n) \tag{4.14a}$$

$$\psi^n - \bar{\psi}^n = (\Delta t/4)(F_2^{n-1/2} - F_2^{n+1/2}) \tag{4.15b}$$

The consistency of (a) with the one-step Crank–Nicholson form (4.11) is evident, the truncation error being $O(\Delta t^2)$. Equation (4.15b) is also consistent with (4.5) since the right-hand term is $O(\Delta t^3)$. We may regard (4.14) either as a scheme to approximate the solution of the compact scheme (4.4) or as an independent scheme to solve the differential equation.

We shall show that this scheme leads to an energy estimate which is consistent with (4.7) to within terms of $O(\Delta t^2)$. Recalling the basic energy argument in (2.11) and the definition of $F_i$ in (4.12) we find

$$\psi \cdot F_1 = \Delta(\phi u^1 \, dS_1) - \mu_1(u^1 u_1)$$
$$\bar{\psi} \cdot \bar{F}_2 = \Delta(\bar{\phi}\bar{u}^2 \, d\bar{S}_2) - \mu_2(\bar{u}^2 \bar{u}_2)$$

so that by multiplying (4.15a) by $\bar{\psi}$ and then using (4.15b) we find

$$\frac{1}{2\,\Delta t}\Delta_t(\psi^n)^2 \tau + [\mu_1(u^1 u_1)^n + \mu_2(\bar{u}^2\bar{u}_2)^n]$$
$$= [\Delta(\phi u^1 \, dS_1) + \Delta(\bar{\phi}\bar{u}^2 \, d\bar{S}_2)] + O(\Delta t^2)$$

Summing over volume elements and noting that $\bar{\psi} = \psi + O(\Delta t^2)$, etc., we again obtain the energy expression (4.7) to within terms $O(\Delta t^2)$. This result is sufficient to enable us to conclude that the ADI scheme converges and furnishes an approximation with the same degree of accuracy as the compact scheme (4.4). This result is independent of any of the fixed ratios $\Delta t/(\Delta x_i)^2$ occurring in either scheme.

To treat the three-dimensional problem, consider in place of (3.14a), etc., the following:

$$\begin{aligned}
\psi^{n+1/4} - \psi^n &= (\Delta t/4)(2F_1^n + F_2^{n+1/4}) \\
\psi^{n+1/2} - \psi^{n+1/4} &= (\Delta t/4)(F_2^{n+1/4} + 2F_3^{n+1/2}) \\
\psi^{n+3/4} - \psi^{n+1/2} &= (\Delta t/4)(F_2^{n+3/4} + 2F_3^{n+1/2}) \\
\psi^{n+1} - \psi^{n+3/4} &= (\Delta t/4)(2F_1^{n+1} + F_2^{n+3/4})
\end{aligned} \tag{4.16}$$

to which the intermediate boundary conditions $\phi^{n+k} = g^{n+k}$, $k = 1/4,\ 1/2,\ 3/4,\ 1$ apply. Then

$$\psi^{n+1} - \psi^n = \Delta t[(F_1^{n+1} + F_1^n)/2 + (F_2^{n+3/4} + F_2^{n+1/4})/2 + F_3^{n+1/2}]$$

so that the scheme is consistent with the Crank–Nicholson form. Also,

$$(\psi^{n+1} + \psi^n)/2 - \psi^{n+1/2} = (\Delta t/4)[(F_1^{n+1} - F_1^n) + (F_2^{n+3/4} - F_2^{n+1/4})]$$

The last pair of equations, which correspond to (4.15) in the two-dimensional case, can provide the basis for an energy argument, although we omit the details here.

## 5. CONCLUSIONS

We have described a finite volume method which closely maintains the parallel between differential and difference arguments. By using intrinsic geometrical properties of the elements, we were able to describe versions of the div, curl, and grad operators, which led, using formal summation by parts techniques, to discrete energy expressions as well as to the identities $\mathrm{div}_h \mathrm{curl}_h \mathbf{u} = 0$ and $\mathrm{curl}_h \mathrm{grad}_h \phi = 0$. The solution of the initial-boundary-value problem for the diffusion equation was described directly in terms of these operators by compact schemes and the resulting energy equations ensured convergence. The schemes could also be simplified to a potential form which can offer computational advantages, and the treatment of general curvilinear coordinates was shown to result from a specialization of these results. Numerical examples validated the second-order accuracy of both $\phi$ and $\mathrm{grad}_h \phi$ which the theory predicts.

## ACKNOWLEDGMENTS

This article reflects valuable insights gained through discussions with colleagues. I mention with particular appreciation T. B. Gatski, D. Gottlieb, H.-O. Kreiss, and G. Strang. This research was sponsored by the National Aeronautics and Space Administration under NASA contract No. NAG-1-812 and by the Air Force Office of Scientific Research under contract No. AFOSR F49620-89-C-0010.

## REFERENCES

Brezzi, F. (1988). A survey of mixed finite element methods, in *Finite Elements: Theory and Applications*, Dwoyer, Hussaini, and Voigt, (eds.), Springer-Verlag, New York, pp. 34–49.

Gatski, T. B., Grosch, C. E., and Rose, M. E. (1989). The numerical solution of the Navier–Stokes equations for three-dimensional, unsteady, incompressible flows by compact schemes, *J. Comput. Phys.* **82**, 298–329.

Kreiss, H. O. (1964). On difference approximations of the dissipative type for hyperbolic equations, *Commun. Pure Appl. Math.* **17**, 335–353.

Lustman, L. R., and Rose, M. E. (1988). A three dimensional calculation of elastic equilibrium for composite materials, *Int. J. Num. Methods Eng.* **26**, 953–971.

Peyret, R., and Taylor, T. D. (1983). *Computational Methods for Fluid Flow*, Springer-Verlag, New York.

Rose, M. E. (1985). A compact finite element method for elastic bodies, *Num. Methods Part. Diff. Eq.* **3**, 209–228.

Rose, M. E. (1983). Compact finite difference schemes for the Euler and Navier–Stokes equations, *J. Comput. Phys.* **49**, 420–442.

Strang, G., and Fix (1973). *An Analysis of the Finite Element Method*, Prentice-Hall, Englewood Cliffs, New Jersey.

Vinokur, M. (1989). An analysis of finite-difference and finite-volume formulations of conservation laws, *J. Comput. Phys.* **81**, 1–52.

Printed by Catherine Press, Ltd., Tempelhof 41, B-8000 Brugge, Belgium

ATTACHMENT #2

# An Implicit Enthalpy Scheme for One-phase Stefan Problems

Milton E. Rose
Department of Mathematics and Computer Science
N.C. A&T State University
Greensboro, NC 27411

**Subject Classifications:**

**Key Words:** Stefan problem, enthalpy method, compact schemes, diffusion equation, ADI techniques.

Running Head: **Enthalpy Scheme for Stefan Problems**

Send proofs to:

Milton E. Rose
4505 Tower Rd.
Greensboro, NC 27410

Tel. 919-294-1783

# An Implicit Enthalpy Scheme for One-phase Stefan Problems*

Milton E. Rose †

## Introduction.

When finite difference equations can be used, ADI schemes provide an effective numerical method to solve multidimensional diffusion equations because they require the solution of simple tridiagonal systems of equations corresponding to a one-dimensional operator at each time step. Although such schemes can be expected to have similar advantages for the treatment of Stefan-type problems, few studies of their application to this class of problems have appeared in the literature. Several studies by White [5,6] have suggested that the treatment of the underlying nonlinear one-dimensional operator which arises in such applications may require a significant number of iterations to converge and may also require a limitation in the time step, thus offering only a moderate improvement over explicit or SOR-type iterative methods. This difficulty apparently arises because standard finite difference operators may not produce a symmetric, positive-definite operator for the Stefan problem.

* This research was sponsored by the Air Force Office of Scientific Research under Contract No. AFOSR F49620-89-C-0010.

† Present address: 4505 Tower Rd. Greensboro, NC 27410

This paper examines a novel enthalpy formulation of one-phase Stefan problems which is suggested by a more general compact finite-volume treatment of diffusion equations (Rose[4]). Limiting our present study to one-dimension, we introduce a discrete operator which is symmetric and, we conjecture, positive-definite and can be solved on a fixed solution domain with a relatively few iterations. The numerical results indicate that the position of the melting front can be determined with first order accuracy by this method, the number of iterations at each time step being determined largely by the number of cells traversed by the front during a time step.

We first review the enthalpy method and a standard finite difference scheme usually associated with the diffusion operator. We then propose a compact finite difference scheme for solving a one-phase Stefan problem and conclude by presenting numerical results for several model problems.

## 1 Enthalpy method.

The one-dimensional Stefan problem involving the enthalpy e, heat flux q, and temperature T is described by the following parabolic system:

$$\begin{aligned} &(a) \quad e_t + q_x = 0 \qquad \text{(conservation of energy)} \\ &(b) \quad q = -\kappa T_x \qquad \text{(Fourier's law)} \\ &(c) \quad T = T(e) \qquad \text{(equation of state).} \end{aligned} \tag{1}$$

in which $\kappa$ is the coefficient of thermal conductivity and a constant unit density is assumed. For ordinary heat conduction problems the equation of state is a one-to-one transformation, in which case e can be eliminated and the familiar heat conduction equation for T results. When melting can occur (involving a latent heat L) the equation of state can be described by the model form

$$\begin{aligned} T-T_0 &= \gamma^+ e, && 0 \le e \\ &= 0, && -L \le e \le 0 \\ &= \gamma^- (e - L), && e \le -L \end{aligned} \tag{2}$$

in which $1/\gamma^{\pm}$ are specific heats and $T_0$ is a a reference temperature which we may assume vanishes, i.e., $T_0 = 0$. (We refer the reader to Crank [1] for a fuller discussion).

In the problem to be discussed below, we will seek to determine (e,q,T) when a slab of material (such as ice) has the initial value e = –L and is subsequently melted by the addition of heat through one or both of its faces (at the endpoints, say, of the unit interval $0 \le x \le 1$) as specified by a linear combination of the temperature and flux. Of particular interest is the position x = s(t) of the interface between the solid and liquid phases. By integrating (1) across this interface we obtain with the use of Gauss' theorem

$$\begin{aligned} &[e]\, s'(t) = [q]\,, \\ &[T] = 0, \end{aligned} \tag{3a}$$

in which [ ] indicates the jump in value across x = s(t). Across the interface, [e] = L and we thus obtain the familiar free boundary conditions

$$\begin{aligned} &L\, s'(t) = [q], \\ &T = 0\,, \qquad x = s(t) \end{aligned} \tag{3b}$$

which were first described by Stefan.

Because (3) is obtained by integrating (1) over a domain including the interface, the solution (e,q,T) can be shown to be a weak-solution of (1) which is smooth in each subdomain separated by the interface. Following a suggestion of Lax concerning conservation laws, such solutions can be expected to result as the weak limits of appropriate discretized forms of (1). In [3], Rose formulated the Stefan problem in the manner described above (enthalpy method) and examined the use of a simple explicit numerical scheme to obtain the solution. (A fuller discussion of this method may be found in Crank [1]).

Let

$$E = 1/2\ d/dt \int_0^1 Te\ dx + \int_0^1 Tq\ dx + Tq\Big|_0^1 ; \qquad (4)$$

represent the total "energy" on the interval. By multiplying (1a) by T, integrating over the fixed interval [0,1] taking account of the energy balance condition (3b) across an interface, and noting the assumption that $T_0 = 0$ we arrive at an "energy balance" equation with the following result:

$$E = T_0\ [q] = 0. \qquad (5)$$

In discussing smooth solutions to the diffusion equation, Rose [4] constructed a finite volume scheme which was consistent with (1) and also satisfied a discrete version of (5). As a result, the scheme could be shown to converge and produce second order accuracy in both T and q. By adapting this scheme to the Stefan problem we expect that an energy result similar to (5) will also emerge, thereby resulting in a symmetric, positive-definite operator which is particularly relevant to the construction of a weak solution to the problem. (Because this scheme can also be interpreted as a non-conforming finite element scheme, the error analysis given by Elliott [2] for the enthalpy method may not be entirely applicable.)

## 2 A standard finite difference scheme.

Consider the two-dimensional diffusion equation

$$u_t = u_{xx} + u_{yy} \tag{4}$$

and let F, G denote standard finite difference approximations to $u_{xx}$ and $u_{yy}$ respectively both involving a spatial parameter $\Delta x$. Using standard finite difference notations, an ADI solution technique to solve (4) is

$$\begin{aligned} &(a) \qquad (u^{n+1/2} - u^{n}) / \tau \quad = F^{n+1/2} + G^{n} \\ &(b) \qquad (u^{n+1} - u^{n+1/2}) / \tau \quad = F^{n+1/2} + G^{n+1} \end{aligned} \tag{5}$$

where $\tau = \Delta t / 2$. This scheme, which is formally second order accurate in both $\Delta t$ and the implied spatial parameter $\Delta x$, is unconditionally stable. The effectiveness of this scheme arises, in part, from the observation that each step involves the solution of a tri-diagonal matrix whose solution can be readily obtained (Thomas algorithm). In one dimension this scheme reduces to the form

$$\begin{aligned} &(a) \qquad (u^{n+1/2} - u^{n}) / \tau \quad = F^{n+1/2} \\ &(b) \qquad (u^{n+1} - u^{n+1/2}) / \tau \quad = F^{n+1/2} \end{aligned} \tag{6}$$

so that in this case only the first step (a) requires the solution of an implicit system of equations.

For a model one-phase problem, $e(x,0) = -L$ initially and we may assume $-L \le e(x,t)$ for $t \ge 0$. If we introduce the notation

$$\begin{aligned} \gamma(e) &= \gamma^{+}, \quad 0 \le e \\ &= 0, \quad -L \le e < 0 \end{aligned} \tag{7a}$$

the equation of state (2) can be written

$$T(e) = \gamma(e)\, e\,, \quad -L \le e \tag{7b}$$

which is the form we shall assume in the following discussion.

Corresponding to (6), a conventional difference scheme arising from (1) is

$$\text{(a)} \quad (e_i^{\,n+1/2} - e_i^{\,n}) / \tau + (q_{i+1/2}^{\,n+1/2} - q_{i-1/2}^{\,n+1/2}) / \Delta x = 0 \tag{8}$$

$$\text{(b)} \quad (e_i^{\,n+1} - e_i^{\,n+1/2}) / \tau + (q_{i+1/2}^{\,n+1/2} - q_{i-1/2}^{\,n+1/2}) / \Delta x = 0$$

with

$$q_i = -\kappa_i (T_{i+1/2} - T_{i-1/2}) / \Delta x, \tag{9}$$

in which $T = T(e)$ is given by (6). As a result, F has the interpretation

$$\begin{aligned} F_i &= [\kappa_{i+1/2}(T_{i+1} - T_i) - \kappa_{i-1/2}(T_i - T_{i-1})] / \Delta x^2 \\ &\equiv \Delta\, (\kappa \Delta T_i) \end{aligned} \tag{10}$$

which is the standard 2nd order difference operator corresponding to $(\kappa u_x)_x$. Here the subscript i has the range [1,M–1], corresponding to a subdivision of the interval (0,1) into M equal subintervals each of length $\Delta x = 1/M$. Thus, for n = 0, 1, 2 ... (8a) leads to a nonlinear system of tridiagonal difference equations

$$e_i^{\,n+1/2} - \tau\, \Delta\, (\kappa \Delta T(e_i^{n+1/2})) = e_i^{n} \tag{11a}$$

With $e_i^{n+1/2}$ so determined, $e_i^{\,n+1}$ can be obtained explicitly from

$$e_i^{\,n+1} = \tau\, \Delta\, (\kappa \Delta T(e_i^{n+1/2})) + e_i^{n+1/2} \tag{11b}$$

As noted earlier, the explicit scheme defined by

$$e_i^{n+1} = \tau \Delta (\kappa \Delta T(e_i^n)) + e_i^n , \qquad n = 0,1,2,...$$

was originally used in [3] to demonstrate the feasibility of the enthalpy method; although it requires the severe stability condition $\Delta t / \Delta x^2 \leq 1/2$ it suggests that the implicit scheme described by (11) may form the basis for an approach to solving the Stefan problem without this stability condition. However, we were not able to develop a satisfactory method to solve this system effectively (c.f. White [5,6]), possibly because the operator in (11a) may fail to be symmetric, positive-definite when (7b) holds . We will now describe a slightly modified descritization method which appears to allow for an effective solution technique.

## 3 A compact finite difference scheme.

If we examine the conventional scheme represented by (7), (8), and (9) we observe that (8) is consistent with the conservation equation (1a) on intervals $\{ x_i - \Delta x/2 \leq x_i \leq x_i + \Delta x/2 \}$ while (9) has been made consistent with Fourier's law (1b) by relating the flux at the endpoints of each such interval to the temperature values $T_i$, $T_{i\pm1}$ related to the centerpoints of an interval and its neighbors. In particular, notice that (9) will provide second order accuracy only if the coefficient $\kappa$ is smooth across subintervals.

We will now describe a slightly different numerical scheme which is suggested by a domain-decomposition argument. With a fixed choice of disjoint subintervals, we propose to describe the physics within each subinterval by solving (1) in isolation from its neighboring intervals (i.e., compactly) and then, separately, extend the solution in the large by means of continuity conditions for e, q, and T across the boundaries of contiguous subintervals. For sufficiently small subintervals, an approximate solution of (1) in each subinterval which satisfies initial and boundary conditions can be obtained by use of a Taylor series. With the addition of the remaining continuity requirements, the result will lead, to a compact discrete approximation of the problem throughout the fundamental domain.

In order to implement this idea for the one-dimensional problem, introduce the M disjoint intervals $\mathcal{I}_i = \{ x_i - \Delta x \le x_i \le x_i + \Delta x \}$, $i = 1, 3, ..., 2M - 1$ as suggested by the stencil

$$| \quad \bullet \quad | \quad \bullet \quad | \quad \bullet \quad |$$
$$x_{i-2} \qquad x_i \qquad x_{i+2}.$$

in which the centerpoints have been indicated by • . First apply the conservation law (1a) in each interval $\mathcal{I}_i$ to obtain the approximate condition

$$\text{(a)} \qquad (e_i{}^{n+1/2} - e_i{}^{n}) / \tau + (q^-_{i+1}{}^{n+1/2} - q^+_{i-1}{}^{n+1/2}) / (2\Delta x) = 0 \tag{12}$$

$$\text{(b)} \qquad (e_i{}^{n+1} - e_i{}^{n+1/2}) / \tau + (q^-_{i+1}{}^{n+1/2} - q^+_{i-1}{}^{n+1/2}) / (2\Delta x) = 0$$
$$i = 1,3,..., 2M-1$$

involving the right and left limits $q^{\pm}$ of the fluxes at the endpoints of the interval $\mathcal{I}_i$ (compare to (8) ). Next, temporarily omitting the superscripts, express Fourier's law (1b) for these flux values by backward and forward differences in the following manner:

$$q^-_{i+1} = -\kappa^-_{i+1} (T^-_{i+1} - T(e_i)) / \Delta x , \tag{13}$$
$$q^+_{i-1} = -\kappa^+_{i-1} (T(e_i) - T^+_{i-1}) / \Delta x.$$

in which $T(e_i)$ is given by the equation of state (7b), viz.,

$$T(e_i) = \gamma(e_i)\, e_i , \quad -L \le e_i \tag{7b}$$

Clearly, (7b), (12), and (13) are consistent with the physical system (1) in each subinterval. In addition, we will impose the following continuity conditions across the endpoints of intervals:

$$[q]_i = [T]_i = 0 \ , \qquad i = 2, 4, ..., 2M-2 \ . \tag{14}$$

Because each interval is fixed in time, these conditions are consistent with the general application of Gauss' theorem across interval endpoints as expressed by (3a).

Following [3], we call the scheme described by (7b), (12), (13), and (14) a compact finite difference scheme to solve (1). Note that the variables which occur are: $(T^{\pm}, q^{\pm})$ at cell endpoints and e at cell centerpoints. The number of variables can be reduced by setting $q = q^+ = q^-$ and also $T = T^+ = T^-$, so that the continuity conditions [q] = [T] = 0 will automatically be satisfied. Thus, except for boundary values, the primary variables can be reduced to the pair (T, q) at cell endpoints and e at cell centerpoints. (For the case of simple heat conduction ($\gamma(e) = 1$) it is a simple matter to show that the system of algebraic equations resulting from (7), (12), (13), and (14) is uniquely determined by the initial and boundary conditions for the discrete problem)

Although the definition of q in (13) by means of one-sided differences might be expected to limit the accuracy of this scheme, the continuity condition [q] = 0 can be seen to lead to

$$\begin{aligned} 0 = [q]_i = \ & -\kappa^-_i(T_{i+1} - T(e_i) / \Delta x) \\ & + \kappa^+_i(T(e_i) - T_{i-1}) / \Delta x \end{aligned} \tag{15}$$

which indicates that these flux values will also provide second order accuracy at interval endpoints which lie interior of the solution domain whenever $\kappa$ is smooth (in this case, a somewhat remarkable fact, proved in [3], is that the one-sided flux values as defined by (13) are also 2nd order accurate at the endpoints of the underlying domain).

If we now let

$$\text{(a)} \qquad F^*_i = -(q_{i+1} - q_{i-1}) / (2\Delta x) \qquad (16)$$

$$= (\kappa^-_{i+1}(T_{i+1} - T(e_i)) - \kappa^+_{i-1}(T(e_i) - T_{i-1})) / (2\Delta x^2)$$

$$i = 1, 3, \ldots, 2M-1,$$

$$\text{(b)} \qquad F^*_i = -[q]_i$$

$$= (\kappa^+_i (T(e_{i+1}) - T_i) - \kappa^-_i (T_i - T(e_{i-1})) / \Delta x$$

$$i = 2, 4, \ldots, 2M-2,$$

then the use of the discretization equations (7b), (12), (13), and (14) leads to the following scheme:

$$\text{(a)} \qquad F^{*\,n+1/2}_i = (e_i^{n+1/2} - e_i^n) / \tau, \qquad i = 1, 3, \ldots, 2M-1$$

$$= 0, \qquad i = 2, 4, \ldots, 2M-2$$

(17)

$$\text{(b)} \qquad F^{*\,n+1/2}_i = (e_i^{n+1} - e_i^{n+1/2}) / \tau, \qquad i = 1, 3, \ldots, 2M-1$$

$$= 0, \qquad i = 2, 4, \ldots, 2M-2$$

in which the variable q has been eliminated. The solution of the tri-diagonal system (17a) yields the values $(T_0, e_1, T_2, e_3, \ldots, e_{2M-1}, T_{2M})^{n+1/2}$. Note that the equations $F^{*\,n+1/2}_i = 0$ occuring in (b) also occur in (a) and are thus redundant in the calculation of the enthalpy values $e_i^{n+1}$ in (17b). The nonlinearity of this system arises directly through the terms $T(e_i)$ in $F_i$.

Following [3], we call (17) the potential form of the compact scheme and it is evident from (16) that F* gives rise to a symmetric operator. A proof (omitted here) that F* is also positive can be given on the basis of energy arguments related to (4), following methods described in [3]. The potential form thus allows us to treat the problem solely in terms of the variables e and T.

## 4 A computational method for the one-phase Stefan problem

In the following we shall assume units such that $\kappa = \gamma = L = 1$. Then $\gamma(e)$ in (7b) has the specific form

$$\begin{aligned} \gamma(e) &= 1, \quad 0 \le e \\ &= 0, \quad -1 \le e < 0 \end{aligned} \tag{18}$$

while (16) reduces to

$$F^*_i = -(T_{i+1} - 2T(e_i) - T_{i-1}) \; / (2\,\Delta x^2) \tag{19a}$$

or else

$$F^*_i = -(T(e_{i+1}) - 2T_i - T(e_{i-1})) \; / \Delta x \tag{19b}$$

depending upon the index i, and in which

$$T(e) = \gamma(e)\, e.$$

We see that (17a) leads to a nonlinear system of tridiagonal difference equations involving (T, e) and to which are to be added boundary conditions involving $T_i^{n+1/2}$ and $q_i^{n+1/2}$ for i = 0, 2M.

For fixed n, if U indicates the unknowns (T, e), the symbolic form of this algebraic system is

$$A(U)\, U = f^n \tag{20}$$

which we propose solving by the iteration scheme: with $U^{(0)} = U^n$, let $U^{(k+1)}$ solve $A(U^{(k)})\, U^{(k+1)} = f^n$, k=0,1,2,.... If convergence occurs, then $U = (T^{n+1/2}, e^{n+1/2})$. Our previous discussion indicates that A(U) is both symmetric and positive-definite and thus satisfies conditions which insure the solvability of (20) by an iteration scheme of this type.

## 5 Numerical experiments.

Figures 1-4 illustrate numerical features of the solution method just described. In the general study a parameter $\sigma$ was used to relate the time step to the mesh by means of $\Delta t = \sigma \Delta x$. The use of a least squares fit to the numerical position of the front verified that the front position was determined with $O(\Delta t)$ accuracy. The average number of iterations required to solve (22) at each time step was in the range 2-4.

The front position was determined as follows: Call a cell (a) partially melted if either, but not both, the left or right endpoint values of T are positive , or (b) completely melted if the centerpoint value $T(e) > 0$. Otherwise, call the cell unmelted. Let

$$\begin{aligned} \delta &= \Delta x \\ &= \Delta x/2 \\ &= 0 \end{aligned} \tag{21}$$

according as the cell is completely melted, partially melted or unmelted. Then $Fr(\delta) = \sum \delta_i$ provides a distance function which can be used to determine the position of the front. (From (19b) we observe that an endpoint value $T > 0$ iff at least one of the contiguous cells having this endpoint in common is a completely melted cell).

I. A front moving with constant speed:

If, initially, $e(x,0) = -1$, then $e(x,t) = \exp(t - x) - 1$ is an analytic solution of a one-phase Stefan problem for a slab whose front moves with the constant speed $s'(t) = 1$ when heated from the left boundary. This example thus allows us to compare the numerical results with known analytic results.

Figures 1a-1c illustrate results for the values: $M = 10$, $\sigma = 1$ so that $\Delta x = \Delta t = 0.1$. The choice of the value $\sigma = 1$ was made in order to examine a situation in which the effects of a dispersion error arising when the front position

does not lie on grid points is absent. The relative errors in the temperature T and the flux q, using $L_2$ error norms, was found to be 6.75 $\times 10^{-4}$ and 8.07 $\times 10^{-3}$ respectively while the relative error of the front position was 5.09 $\times 10^{-20}$. The average number of iterations per time step was 2.75. The cause of the oscillation in the q-error in Fig.1c will be examined shortly.

For M = 20, $\sigma = 1$, so that $\Delta x = \Delta t = 0.05$., the relative errors in the temperature T and the flux q were 1.79 $\times 10^{-4}$ and 3.92 $\times 10^{-3}$ , respectively, while the relative error of the front position was negligible. The average number of iterations per time step in this case was 2.875.

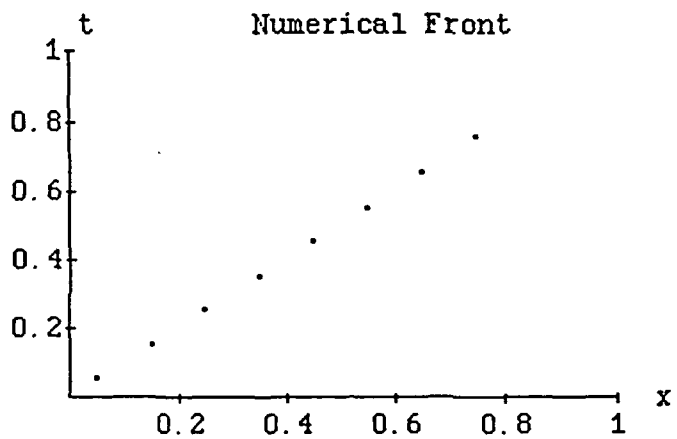


Figure 1a. Plot of the numerically calculated front position ($\sigma = 1$).

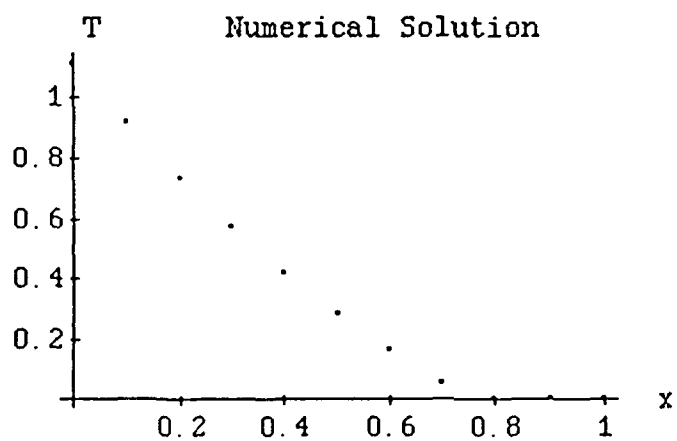


Figure 1b. Plot of the corresponding numerical temperature T

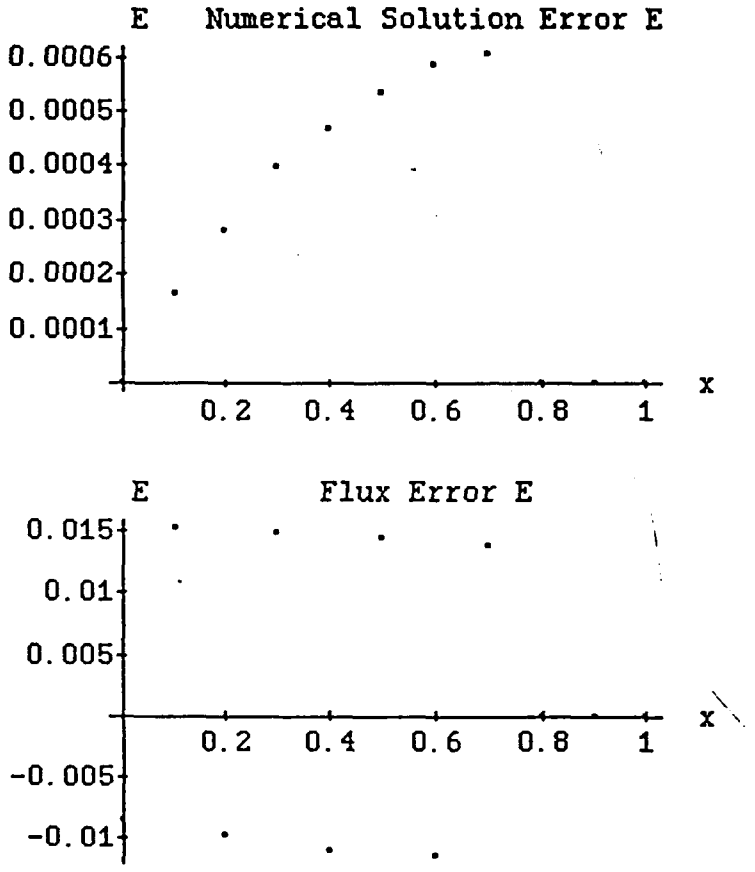


Figure 1c. Plots of the numerical errors of T and q (observe the oscillation in the q error).

Finally, Figure 1d illustrates the front positions when $\Delta x = 0.1$, $\Delta t = 0.05$,.which corresponds to $M = 10$, $\sigma = 0.5$. The relative error norm of the front was 0.0542, the corresponding error norms for T and q were $8.94 \times 10^{-3}$ and $4.16 \times 10^{-2}$, respectively, and the average numer of iterations per time step was 2.31. As a result, we can expect that the dispersion error arising from the use of a fixed grid when a front with variable speed occurs will reduce the overall accuracy. However, for this and the problems considered below we found the accuracy of the front position to be at least $O(\Delta t)$.

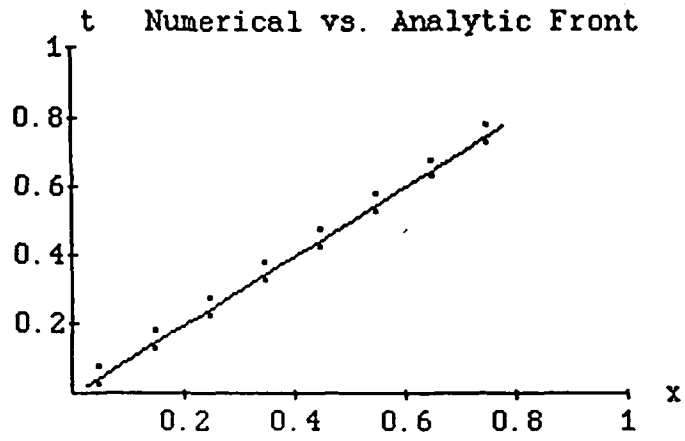


Figure 1d. Numerical front when $\sigma = 0.5$.

2. The slab, cylinder and sphere heated with a constant flux $q(1,t) = -1$.

The preceding results suggest that the parameter $\sigma$ may influence the accuracy when the front speed is variable. This situation arises in the following examples.

Figures 2-4 illustrate numerical results obtained for various geometries when a constant flux of heat is added through at boundary $x = 1$, $q(1,t) = -1$, while $q(0,t) = 0$. The initial position of the front is $s(0) = 1$. In all cases, $\sigma = 1$. The average number of iterations per time step was: slab = 2.68, cylinder = 3.46, sphere = 3.33.

Slab

Figure 2a shows a least squares fit of the form

$$s(t) = 0.988 - 0.883\ t + 0.118\ t^2$$

to the numerically determined front. The solution plots in Figures 2b-2c are at a time slightly after the time of the final front position indicated in Figure 2a..

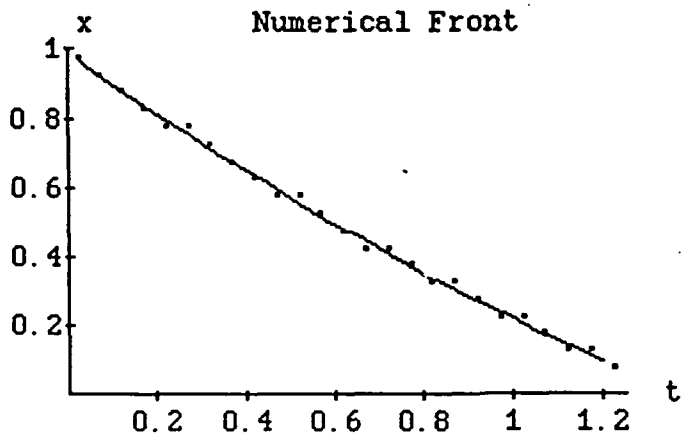


Figure 2a. A least squares fit to the numerical front for a slab geometry.

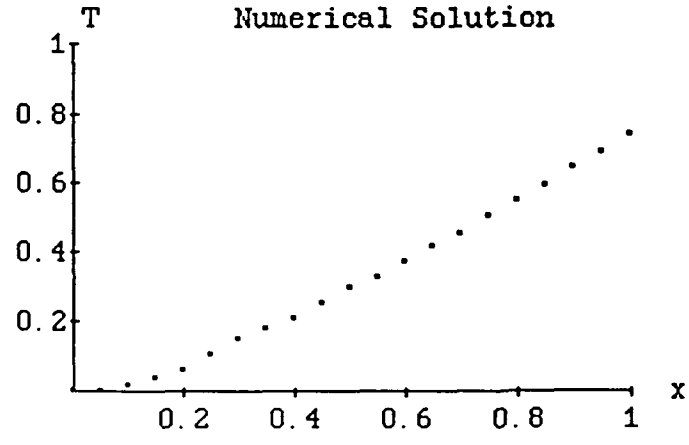


Figure 2b. The numerical temperature T for a slab geometry.

## Cylinder

The front positions resulting in the complete melting of a cylinder indicated in Figure 3a has been fitted with the cubic polynomial

$$s(t) = 1.02 - 1.46\,t + 1.78\,t^2 - 3.38\,t^3.$$

The solution plots in Figures 3b shows the numerical temperature T prior to the time complete melting.has occurred.

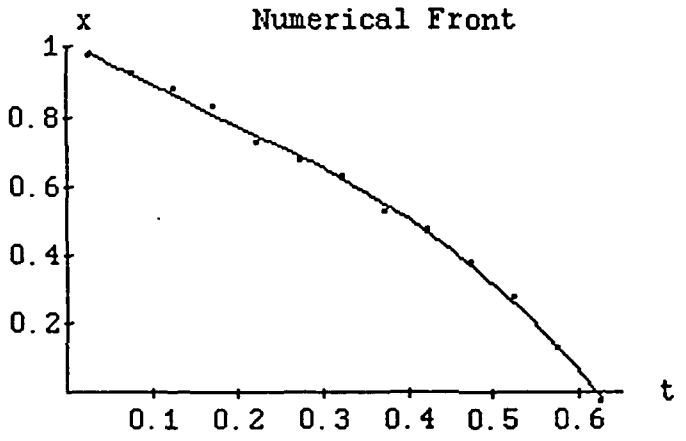


Figure 3a. A least squares fit to the numerical front for a cylinder.

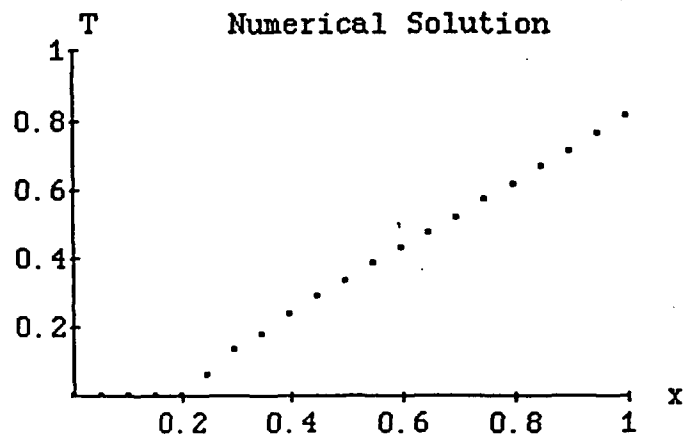


Figure 3b. The numerical temperature for a cylinder at a time shortly before complete melting.

## Sphere

The cubic

$$s(t) = 1.02 - 1.36\,t + 1.31\,t^2 - 2.80\,t^3.$$

fits the data indicated in Figure 4a. The slight irregularity of the solution which is illustrated in Figure 4b appears to be due to a reflection arising from the free boundary at $x = s(t)$. The numerical flux (Fig. 4c) appears to be a sensitive indicator of this irregularity.

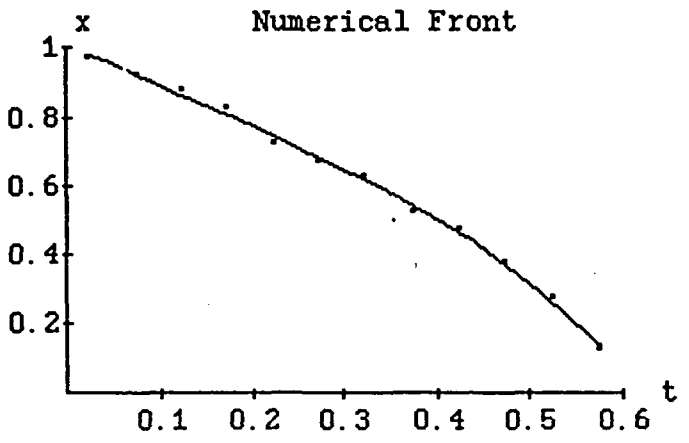


Figure 4a. A least squares fit to the numerical front for a sphere.

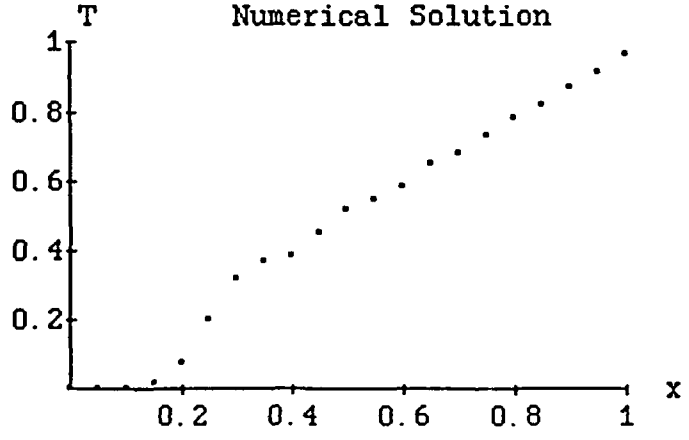


Figure 4b. The numerical temperature for a sphere at a time shortly before complete melting. Note the evidence of an inaccuracy behind the front.

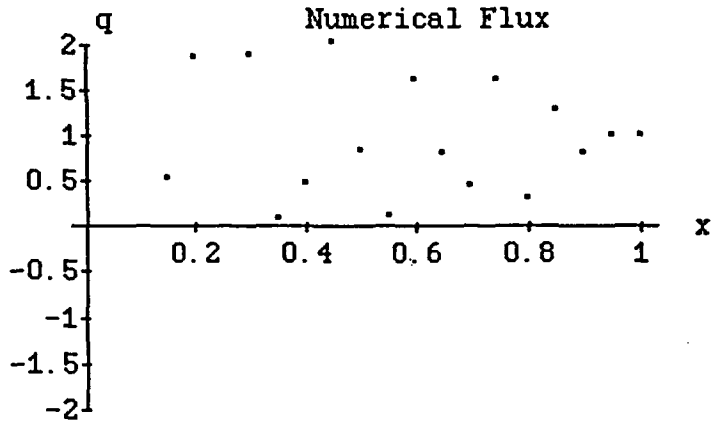


Figure 4c. The numerical flux corresponding to Fig. 4b.

## The parameter σ

As suggested above, the choice of the parameter $\sigma = \Delta t/\Delta x$ can be expected to affect the dispersive error arising whenever the speed of the front differs from $1/\sigma$. The following figures help illustrate this fact by comparing the results for the sphere shown in Fig. 4 (in which $\sigma = 1$) with similar results when $\sigma = 0.2$. Figs. 5b-5c indicate that this choice of $\sigma$ results in a substantially smoother approximation and leads us to conjecture that a CFL-type condition of the form

$$\sigma \| s' \| \leq 1 \tag{22}$$

is required to insure smoothness, rather than stability, for this method.

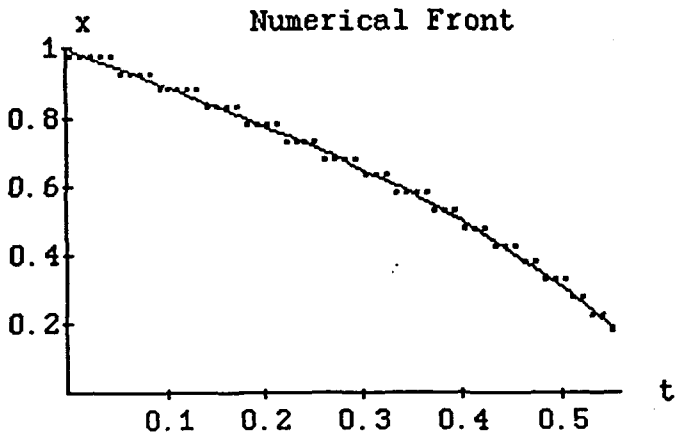


Figure 5a. Numerical front for the sphere when $\sigma = 0.2$

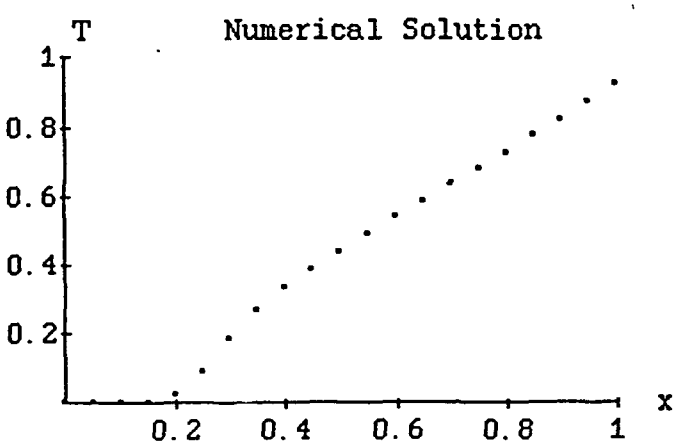


Figure 5b. Numerical temperature for the sphere when $\sigma = 0.2$. showing a partial elimination of the irregularity behind the front (compare Figure 4b).

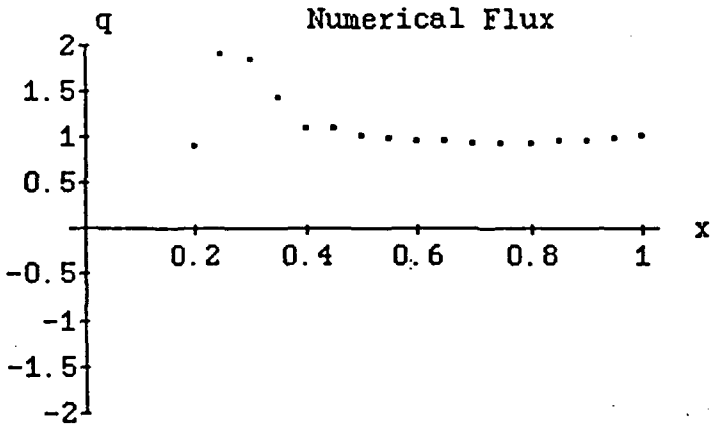


Figure 5c. Partial smoothing of the numerical flux when $\sigma = 0.2$ (compare to Fig. 4c).

## Concluding Remarks:

These results indicate that the 1D, one-phase Stefan problem can be treated by the enthalpy method using an unconditionally stable numerical method which requires the iterative solution of a symmetric (positive-definite) tridiagonal system of equations (21) at each time step. Because the number of iterations per time step is relatively small (< 4 for each of the cases treated), this provides a computationally efficient method. Also, because this same basic structure underlies the use of ADI solution techniques it suggests that multidimensional problems can be treated in a similar manner.

Further studies are required to understand the mechanisms which give rise to numerical irregularities when the front moves relative to a fixed mesh and which appear to be controlled by the parameter $\sigma = \Delta t/\Delta x$. Other aspects of this problem can be expected to appear in higher dimensions.

Finally, in view of the fact that discrete "energy" estimates similar to those available for smooth solutions as described by eq.(5) can be given for the scheme described here (following developments given in Rose [4]), the possibility exists of developing a more complete theoretical analysis of the enthalpy method based on this observation. In particular, this would prove that the basic operator arising from the scheme is, indeed, positive definite, a fact that was not shown in this paper.

# References

1. Crank, John, (1984) *Free and moving boundary problems*, Oxford University Press

2. Elliott, C.M., (1987) *Error analysis of the enthalpy method*, IMA J. Numer. Anal., **7**, 61-71.

3. Rose, Milton. E., (1960). *Math. Comput.*, **14**, 249-56

4. _____(1989). *J. Sci. Comput.*, **4**, No.3

5. White, R. E., (1982). *SIAM J.Numer. Anal.*, **19**, 1129-1157

6._____ (1983). *Math. Comput.*, **41**, No.164, 337-347

ATTACHMENT #3

# A COMPACT FINITE VOLUME SCHEME FOR 2-D STEFAN PROBLEMS AND VECTOR/MULTIPROCESSOR COMPUTERS.

Robert E. White
Department of Mathematics
N. C. State University
Raleigh, N. C.

Bolindra N. Borah
Department of Mathematics and Computer Science
N. C. A&T State University
Greensboro, N. C.

Archimedes J. Kyrillidis
Department of Mathematics and Computer Science
N. C. A&T State University
Greensboro, N. C.

# A COMPACT FINITE VOLUME SCHEME FOR 2-D STEFAN PROBLEMS AND VECTOR/MULTIPROCESSOR COMPUTERS.*

Robert E. White
Department of Mathematics
N. C. State University
Raleigh, N. C.

Bolindra N. Borah
Department of Mathematics and Computer Science
N. C. A&T State University
Greensboro, N. C.

Archimedes J. Kyrillidis
Department of Mathematics and Computer Science
N. C. A&T State University
Greensboro, N. C.

**Abstract.** We consider both the compact finite volume and finite difference space discretizations of the Stefan problem. The resulting algebraic systems are solved by nonlinear versions of ADI and SOR. Both algorithms contain significant parallelism which is demonstrated on two vector/multiprocessing computers, the Alliant FX/40 and the Cray Y-MP. Numerical experiments indicate that the compact discretization and ADI give the best accuracy with the minimum computational cost.

* This research was sponsored by the Air Force Office of Scientific Research, Bolling Air Force Base, D. C. Contract No. F49620-89-C-0010 and Army Research Office, Research Triangle Park, N. C. Contract No. DAAL03-90-G-0126.

# A COMPACT FINITE VOLUME SCHEME FOR 2-D STEFAN PROBLEMS AND VECTOR/MULTIPROCESSOR COMPUTERS.

**1. Introduction.** This report outlines some new numerical methods for the solution of multiple space dimension Stefan problem. This will include both SOR and ADI algorithms for the nonlinear algebraic systems which result from both the FDM and compact space discretizations methods. Analysis of convergence will be discused.

The ADI algorithms have been introduced because they appear, in many examples, to be more effective than some of the traditional algorithms related to the Stefan problem. Moreover, these ADI algorithms, as in the linear parabolic problems, have large number of independent tridiagonal solvers. Therefore they can be effectively implemented on vector/multiprocessing computers. This is illustrated for Alliant FX/40 and the Cray Y-MP.

In this paper, we will use the enthalpy formulation of the Stefan problem. (See Rose [3], Elliot [2] and White [5]).

$$
\begin{aligned}
& E_t - \Delta\beta(E) = f \text{ on } D \times (0,T) \\
& E(x,0) = \text{ given on } D \\
(1) \qquad & \beta(E(x,t)) = \text{ given on } \partial D \times (0,T), \\
\text{where} \qquad & \beta(E) = \text{Kirchoff transformed temperature}
\end{aligned}
$$

$\beta(E) = u$ is the "inverse" of the enthalpy function $E = H(u)$.

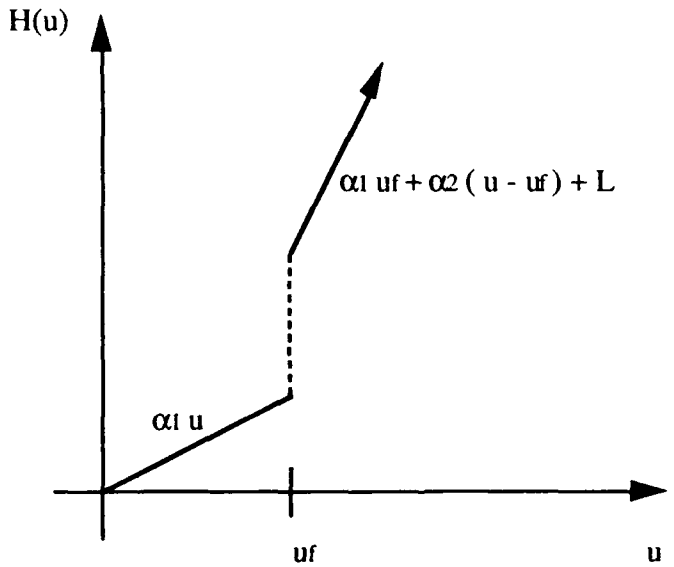

Both (8.1) and (8.2) can be solved as in (5). For example, consider (8.1) with $k + 1/2$ suppressed and m equals the iteration index.

Consider

$$(\alpha I + \hat{H}(E))\, E = d \tag{9}$$

$$E^{m+1} = (\alpha I + \hat{H}(E^m))^{-1} d$$

$$= (I + \frac{1}{\alpha} \hat{H}(E^m))^{-1} \alpha^{-1} d \tag{10}$$

Proposition 1:

Let A, A(E), $\hat{H}(E)$, $\hat{V}(E)$ be as above. If A is an M-matrix and $\beta(E)$ is as defined above, then A(E), $\hat{H}(E)$, $\hat{V}(E)$ are non-singular for small $\Delta t$. Moreover, there exists $\alpha_0 > 0$ such that for $\alpha \geq \alpha_0$ (10) converges to the unique solution of (9).

The proof follows that given in White [6] for (4) and (5).

In practice $\alpha$ is used as an acceleration parameter and usually only 3-5 iterations are required to solve (8.1) or (8.2). The schemes in (8.1) and (8.2) do not solve the implicit time step:

$$\frac{E^{k+1} - E^k}{\Delta t} + A(E^{k+1})\, E^{k+1} = f^{k+1} \tag{11}$$

For each fixed problem in (11) there are a number of ADI schemes with multiple H and V sweeps. We focus on only one in the next section.

**3. ADI: Multiple H and V sweeps per time step.** Consider the simple nonlinear system (4) with

$$A(E) = \overline{H}(E) + \overline{V}(E), \quad \text{or}$$

$$(\hat{H}(E) + \hat{V}(E))\, E = d \tag{12}$$

After linearization the multiple H and V sweep ADI algorithm is

$$(\alpha I + \hat{H}(E^{m_0}))\, E^{m+1/2} = d + (\alpha I - \hat{V}(E^{m_0}))\, E^m \tag{13.1}$$

$$(\alpha I + \hat{V}(E^{m_0}))\, E^{m+1} = d + (\alpha I - \hat{H}(E^{m_0}))\, E^{m+1/2} \tag{13.2}$$

One can solve (13.1) and insert it into (13.2) to obtain

$$E^{m+1} = \delta(E^{m_0}) + \mathfrak{H}(E^{m_0})\, E^m \tag{14}$$

If $E^{m+1}$ converges, define $E^{m_0+1}$ to be the limit

$$E^{m_0+1} = \delta(E^{m_0}) + \mathfrak{H}(E^{m_0})\, E^{m_0+1}$$

provided the spectral radius of $\mathfrak{H}(E^{m_0})$ is less than 1. This is

$$E^{m_0+1} = (I - \mathfrak{H}(E^{m_0}))^{-1}\, \delta(E^{m_0}) \tag{15}$$

Line (15) forms the outer iteration of our algorithm to solve (2).

Proposition 2:

Consider (12) and the algorithms (13) - (15). Let the same assumptions hold as in proposition 1. Then there exists a $\overline{\alpha_0} > 0$ such that if $\alpha \geq \overline{\alpha_0}$, then the inner iterations (14) converges to $E^{m_0+1}$ in (15), and $E^{m_0+1}$ in (15) converges to thr solution in (12).

The proof requires the spectral radius of $\mathfrak{H}(E)$ to be uniformly bounded below 1.0. This step makes use of monotonicity properties (nonnegative matrices), and it contrasts with the linear case where symmetric positive definite matrices are used.

The above schemes is not the only way to do multiple H and V sweeps, but it does allow one to give a convergence analysis. The best version of multiple H and V sweeps is not yet clear. The numerical experiments that we have done indicate that the Peaceman-Ranchford method (one H and V sweep per time step) is adequate.

**4. Numerical Experiments.** In this section we consider the numerical solution of

$$E_t - \Delta\beta(E) = 0, \text{ where the domain } D = (0,1) \times (0,T), \; T = \frac{1}{\sqrt{2}}$$

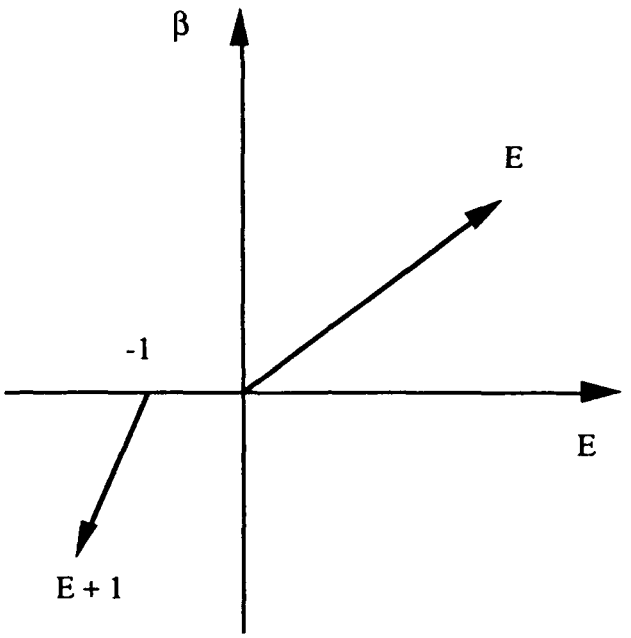


$$\text{and } E = \begin{cases} e^{t - \frac{1}{\sqrt{2}}(x+y)} - 1, & t - \frac{1}{\sqrt{2}}(x+y) \geq 0 \\ -1, & t - \frac{1}{\sqrt{2}}(x+y) < 0 \end{cases}$$

The space variables are discretized in two ways, the compact finite volume (CPT) (See Rose [4]), and the traditional five-point finite difference method (FDM). The resulting algebraic problems are solved by ADI (one H and V sweep per time step) and by SOR. The computations were done on two vector/multiprocessing computers: the Alliant FX/40 and the Cray Y-MP. The Alliant FX/40 has two processors each with a vector pipeline. The Cray Y-MP was used as a single processor with a more sofisticated vector pipeline and much shorter clock cycle time (4 nsec as compared to 170 nsec).

The CPT space discretization has a great deal of parallelism wich can be executed on either vector pipelines or multiprocessing architectures. The unknowns at the center of the cells maybe grouped together, and the unknowns at the boundary of the cells grouped together. The resulting coefficient matrix has the form of a two coloring scheme. Hence one can execute the SOR scheme for the CPT discretization on vector pipelines. Also the CPT space discretization when solved by

ADI methods will have a large number of independent tridiagonal solvers. Thus, the vector version of the tridiagonal algorithm may be used.

In the case of FDM space discretization, the traditional red-black ordering of nodes allows vectorization of the SOR algorithm. Also, domain-decomposition methods have been used on SOR so that the two processors of the Alliant FX/40 can be effectively used. Of course, we can use the vector version of the tridiagonal algorithm to solve the FDM when ADI is used.

| Computers \ Cells | $16^2$ | $32^2$ | $64^2$ |
|---|---|---|---|
| Alliant, serial | 2.01 | 15.64 | 122.28 |
| Alliant, vector | 1.02 | 5.98 | 38.63 |
| Alliant, vector, 2 processors | 0.57 | 3.32 | 21.07 |
| Cray, serial | 0.129 | 0.89 | 6.52 |
| Cray, vector | 0.062 | 0.32 | 1.76 |

Table 1: CPT-ADI

| Computers \ Cells | $16^2$ | $32^2$ | $64^2$ |
|---|---|---|---|
| Alliant, serial | 4.68 | 74.44 | 1155.00 |
| Alliant, vector | 2.67 | 30.72 | 508.81 |
| Alliant, vector, 2 processors | 1.41 | 15.99 | 270.91 |
| Cray, serial | 0.41 | 6.23 | 96.24 |
| Cray, vector | 0.11 | 1.06 | 11.34 |

Table 2: CPT-SOR

Table 1 contains computing time done for the compact discretization and using one sweep ADI algorithm. Both computers were effective vectorizers. Table 2 contains computing times done for the compact discretizatin with red-black ordering SOR algorithm where $\omega = 1.2$.

| Computers \ Cells | $16^2$ | $32^2$ | $64^2$ |
|---|---|---|---|
| Alliant, serial | 0.82 | 12.93 | 186.72 |
| Alliant, vector | 0.89 | 10.29 | 124.97 |
| Alliant, vector, 2 processors | 0.51 | 5.58 | 67.35 |
| Cray, serial | 0.069 | 1.05 | 15.48 |
| Cray, vector | 0.043 | 0.42 | 4.19 |

Table 3: FDM-SOR

The third table contains computing times for the FDM with red-black ordering for SOR where $\omega = 1.2$. This method requires more iterations to reach convergence than does the CPT-SOR method.

All three methods give good accuracy. The CPT-ADI seems to be more accurate and less computing time required for this and related examples.

## References


1. D. R. Athey, "A finite difference scheme for melting problems", J. Inst. Math Appl., vol. 13 (1974), pp. 353-366

2. C. M. Elliot, "On the finite element approximation of elliptic variational inequality arising from an implicit time discretization of the Stefan problem", IMA J. Num. Analy., vol. 1 (1981), pp. 115-125

3. M. E. Rose, "A method for calculating solutions of parabolic equations with free boundary", Math. Comp., vol. 14 (1960), pp. 249-256

4. M. E. Rose, "Compact finite volume methods for the diffusion equations", J. Sci. Comp., vol 4, no. 3 (1989), pp. 261-290

5. R. E. White, "A numerical solution of the enthalpy formulation of the Stefan problem", SIAM J. of Num. Analy., vol. 19 (1982), pp. 1158-1173

6. R. E. White, "A modified finite difference scheme for the Stefan problem", Math. of Comp., vol. 41, no. 164 (Oct., 1983), pp. 337-347

7. M. A. Williams and D. G. Wilson, "Iterative solution of a nonlinear system arising in phase-change problems", SIAM J. Sci. Comp., vol. 11, no. 6 (Nov., 1990), pp. 1087-1101

ATTACHMENT #4

# A COMPARATIVE STUDIES OF COMPACT FINITE VOLUME METHODS FOR THE 2-D DIFFUSION EQUATION WITH FINITE DIFFERENCE ADI AND SOR.

Bolindra N. Borah
Department of Mathematics and Computer Science
N. C. A&T State University
Greensboro, N. C.

Robert E. White
Department of Mathematics
N. C. State University
Raleigh, N. C.

Archimedes J. Kyrillidis
Department of Mathematics and Computer Science
N. C. A&T State University
Greensboro, N. C.

# A COMPARATIVE STUDIES OF COMPACT FINITE VOLUME METHODS FOR THE 2-D DIFFUSION EQUATION WITH FINITE DIFFERENCE ADI AND SOR.*

Bolindra N. Borah
Department of Mathematics and Computer Science
N. C. A&T State University
Greensboro, N. C.

Robert E. White
Department of Mathematics
N. C. State University
Raleigh, N. C.

Archimedes J. Kyrillidis
Department of Mathematics and Computer Science
N. C. A&T State University
Greensboro, N. C.

**Abstract.** Recently developed Compact Finite Difference scheme (CPT) is applied to two dimensional diffusion equations. The relative merits of CPT-ADI are investigated with other computational schemes such as finite difference method - ADI (FDM-ADI) and FDM-SOR. The numerical results obtained from these three approaches are compared to known analytical solutions. The primary interest of this study lies on vectorization and parallel processing. According to our results shown in tables 1, 2 and 3, CPT-ADI is found to be superior scheme with regards to accuracy, than both FDM-ADI and FDM-SOR. It is also fastest algorithm than both FDM-ADI and FDM-SOR as it is evident from CPU times.

* This research was sponsored by the Air Force Office of Scientific Research, Bolling Air Force Base, D. C. Contract No. F49620-89-C-0010 and Army Research Office, Research Triangle Park, N. C. Contract No. DAAL03-90-G-0126.

# A COMPARATIVE STUDIES OF COMPACT FINITE VOLUME METHODS FOR THE 2-D DIFFUSION EQUATION WITH FINITE DIFFERENCE ADI AND SOR.

**1. Introduction.** We shall describe briefly the compact finite difference method (CPT) for one dimmensional steady state problem. The extension to 2-D problem may be easily done. The underlying physics behind this approach lies in solving the differential equation in isolation from its neighboring subintervals (i.e. compactly). Then, extend the solution in the large by means of continuity conditions for the flux and temperature accross the boundaries of the contiguous subintervals.

We consider here one dimensional steady diffusion problem:

(1) D. E. $u' = f$

(2) $\phi' = u$

(3) B. C. $\phi = g$

for $x \in I$ and $I = [I_-, I_+]$.

Divide the interval I into m nonoverlaping subintervals:

$$I_j = \left\{ x \mid x_{j-\frac{1}{2}} \le x \le x_{j+\frac{1}{2}} \right\},$$

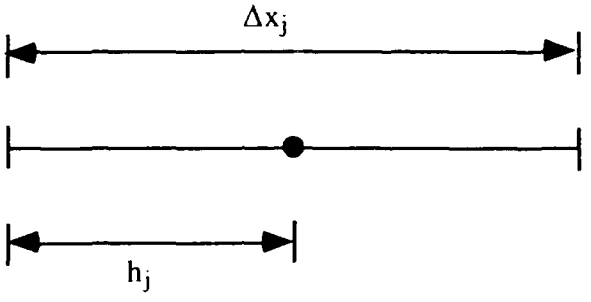


$(\Delta x_j = 2\, h_j)$

with center points $x_j$, $j = \frac{1}{2}, \frac{3}{2}, \ldots, M - \frac{1}{2}$ and interior endpoints $x_j$, $j = 1, 2, \ldots, M - 1$. We shall adopt the finite difference notations $\Delta x_j = x_{i+\frac{1}{2}} - x_{i-\frac{1}{2}}$, $h_i = \frac{\Delta x}{2}$ and $u(i) = u_i$. We also denote:

$$I_c = \left\{ \frac{1}{2}, \frac{3}{2}, \ldots, M - \frac{1}{2} \right\} \text{ (center points)}$$

$$I_e = \{1, 2, \ldots, M - 1\} \text{ (interior endpoints)}$$

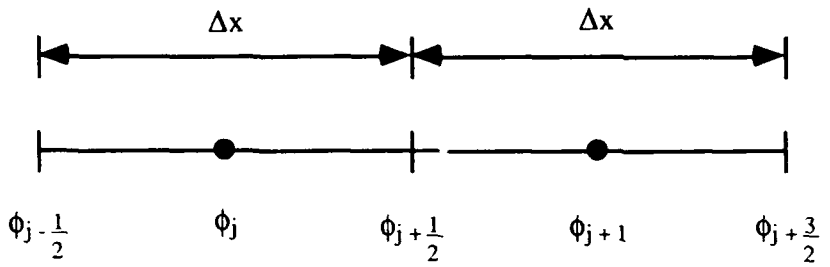


Fig. 1.

The discrete equations for (1) and (2) can be written as, for $j \in I_c$,

(4) $$u_{j+\frac{1}{2}} - u_{j-\frac{1}{2}} = \Delta x_j f_j$$

(5 a) $$\phi_{j+\frac{1}{2}} - \phi_j = h_j u_{j+\frac{1}{2}}$$

(5 b) and $$\phi_j - \phi_{j-\frac{1}{2}} = h_j u_{j-\frac{1}{2}}$$

Next, it is required that both u and $\phi$ be continuous across every endpoint common to two intervals:

$$[u]_i = [\phi]_i = 0 \quad \text{for } i \in I_e.$$

Using this continuity condition $[u]_i = 0$ in terms of $\phi$ we have

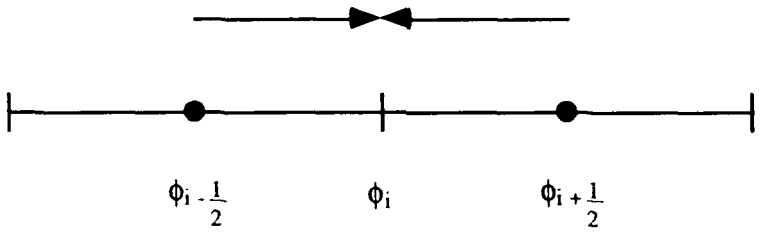


$$\frac{\phi_i - \phi_{i-\frac{1}{2}}}{h_{i-\frac{1}{2}}} = \frac{\phi_{i+\frac{1}{2}} - \phi_i}{h_{i+\frac{1}{2}}}$$

and in the case of equal intervals, which reduces to

(6) $$\phi_i = \frac{\phi_{i+\frac{1}{2}} + \phi_{i-\frac{1}{2}}}{2}, \quad i \in I_e \quad \text{(endpoints)}$$

Now from (4) and (5) we get,

(7 a) $$\phi_{j+\frac{1}{2}} - 2\,\phi_j + \phi_{j-\frac{1}{2}} = 2\,h_j^2\,f_j, \quad i \in I_c$$

and from (6)

(7 b) $$\phi_{j+\frac{1}{2}} - 2\,\phi_j + \phi_{j-\frac{1}{2}} = 0, \quad i \in I_e$$

The equations (7) and the boundary conditions lead to determined system of algebraic equations for the values of $\phi$. These equations lead to a tridiagonal system of equations which is, therefore, solved by Thomas algorithm.

The extension to two dimensional scheme may be easily done. Two dimensional stencil is shown in Fig. 2.

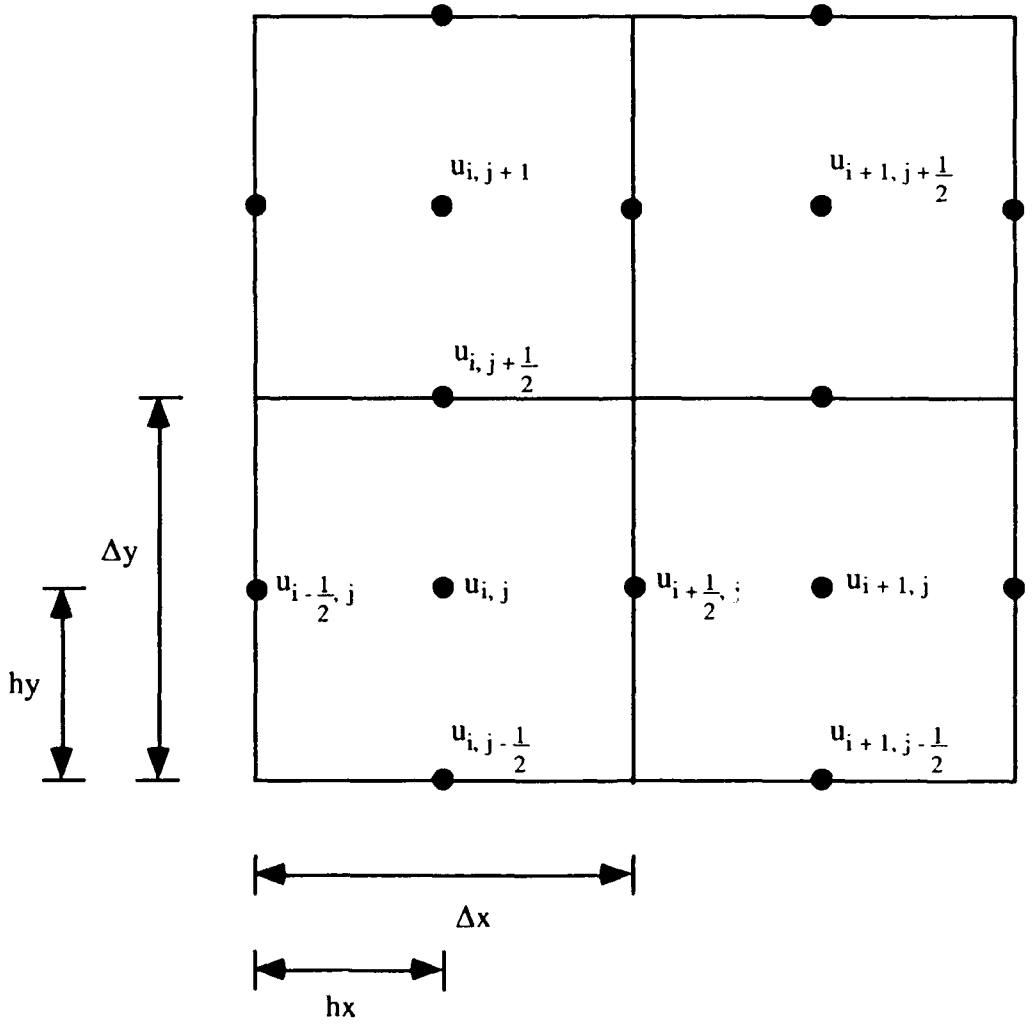


Fig. 2.

Consider the two dimensional diffusion equation $u_t = u_{xx} + u_{yy}$. The compact ADI method is given by lines (8) - (12):

(8 a) $$\frac{u_{i,j}^{n+\frac{1}{2}} - u_{i,j}^{n}}{\tau} = F_{i,j}^{n+\frac{1}{2}} + G_{i,j}^{n}$$

(8 b) $$\frac{u_{i,j}^{n+1} - u_{i,j}^{n+\frac{1}{2}}}{\tau} = F_{i,j}^{n+\frac{1}{2}} + G_{i,j}^{n+1}$$

where $F_{i,j}$ and $G_{i,j}$ are standard finite difference expressions for $u_{xx}$ and $u_{yy}$ respectively and $\tau = \frac{\Delta t}{2}$. Now

(9 a) $$F_{i,j}^{n+\frac{1}{2}} = \frac{-\left[q_{i+1,j}^{n+\frac{1}{2}} - q_{i-1,j}^{n+\frac{1}{2}}\right]}{2\,\Delta x}$$

(9 b) $$G_{i,j}^{n} = \frac{-\left[q_{i,j+1}^{n} - q_{i,j-1}^{n}\right]}{2\,\Delta y}$$

Notice that we modify the indices from the previous discusion. From Fourier law we have $q = -\kappa\, u_x$, therefore

(10 a) $$q_{i+1,j}^{n+\frac{1}{2}} = \frac{-\kappa_{i+1,j}\left[u_{i+1,j}^{n+\frac{1}{2}} - u_{i,j}^{n+\frac{1}{2}}\right]}{\Delta x}$$

(10 b) $$q_{i-1,j}^{n+\frac{1}{2}} = \frac{-\kappa_{i-1,j}\left[u_{i,j}^{n+\frac{1}{2}} - u_{i-1,j}^{n+\frac{1}{2}}\right]}{\Delta x}$$

(10 c) $$q_{i,j+1}^{n} = \frac{-\kappa_{i,j+1}\left[u_{i,j+1}^{n} - u_{i,j}^{n}\right]}{\Delta y}$$

(10 d) $$q_{i,j-1}^{n} = \frac{-\kappa_{i,j-1}\left[u_{i,j}^{n} - u_{i,j-1}^{n}\right]}{\Delta y}$$

Assuming $\kappa = 1$ and $\Delta x = \Delta y$, we have from (8) with the help of (9) and (10)

(11) $$-u^{n+\frac{1}{2}}_{i-1,j} + (\alpha + 2)\, u^{n+\frac{1}{2}}_{i,j} - u^{n+\frac{1}{2}}_{i+1,j} = u^{n}_{i,j-1} + (\alpha - 2)\, u^{n}_{i,j} - u^{n}_{i,j+1}$$

$$i, j = 1, 3, \ldots, 2M - 1, \quad \alpha = \frac{4(\Delta x)^2}{\Delta t}, \quad \Delta x = \Delta y$$

(12) $$-u^{n+1}_{i,j-1} + (\alpha + 2)\, u^{n+1}_{i,j} - u^{n+1}_{i,j+1} = u^{n+\frac{1}{2}}_{i-1,j} + (\alpha - 2)\, u^{n+\frac{1}{2}}_{i,j} - u^{n+\frac{1}{2}}_{i+1,j}$$

$$i, j = 1, 3, \ldots, 2M - 1$$

and the continuity conditions are

(11 a) $$-u^{n+\frac{1}{2}}_{i-1,j} + 2\, u^{n+\frac{1}{2}}_{i,j} - u^{n+\frac{1}{2}}_{i+1,j} = 0$$

$$i, j = 2, 4, \ldots, 2M - 2$$

(12 a) $$-u^{n+1}_{i,j-1} + 2\, u^{n+1}_{i,j} - u^{n+1}_{i,j+1} = 0$$

$$i, j = 2, 4, \ldots, 2M - 2$$

The two algebraic systems (11), (11a), and (12), (12a) can be solved by the tridiagonal algorithm.

**2. Numerical experiments.** One of the primary objectives of this project is to vectorization of 1-D and 2-D diffusion problems. We vectorize the 2-D heat equation for the Cray Y-MP using red-black SOR algorithm.

We consider three analytical solutions for the following diffusion equation and compare them with respective numerical solutions. The results are recorded in tables 1, 2 and 3.

The two dimensional diffusion equation is $u_t = u_{xx} + u_{yy} + f(x,y,t)$, $0 < x < 1$, $0 < y < 1$, $t > 0$. The following analytical solutions are considered:

(a) $u(x, y, t) = \exp\{t - x\cos\theta - y\sin\theta\}$, $\theta$ being any angle, however, $\theta = 0, \pi/2$ reduce the problem into an one dimensional one. We use $f = 0$ and $\theta = \pi/4$.

(b) $u(x, y, t) = 2t + x^2\cos^2\theta + y^2\sin^2\theta$, $\theta$ being any angle, $f = 0$.

(c) $u(x, y, t) = x(1 - x)\, y(1 - y)e^{-t}$, and $f(x, y, t) = (x(1 - x)(2 - y(1-y)) + 2y(1-y))e^{-t}$.

All the problems mentioned above are associated with Dirichlet boundary conditions.

The CPT-ADI is compared with FDM-ADI and FDM-SOR. The functional errors in each of the three methods are of $O(h^2)$ as expected and derivative errors are of $O(h)$. The results are shown in table 1, table 2 and table 3.

FDM-ADI $\Delta t = (\Delta x)^2$

| No. of hx = hy cells | No. of iterations | CPU time (sec) | Max function error | Max derivative error |
|---|---|---|---|---|
| 8 | 32 | 0.2834 | 2.07583E-2 | 1.055968E-1 |
| 16 | 128 | 4.45 | 6.48407E-3 | 5.343229E-2 |
| 32 | 512 | 69.65 | 1.826602E-3 | 2.889879E-2 |
| 64 | 2048 | 1105.48 | 8.967522E-4 | 1.5545622E-2 |

CPT-ADI $\Delta t = \Delta x$

| No. of hx = hy cells | No. of iterations | CPU time (sec) | Max function error | Max derivative error |
|---|---|---|---|---|
| 8 | 8 | 0.15 | 9.359392E-5 | 1.9731343E-3 |
| 16 | 16 | 1.0 | 2.366787E-5 | 6.054254E-4 |
| 32 | 32 | 7.567 | 5.9340348E-6 | 2.120109E-4 |
| 64 | 64 | 58.8 | 1.4842674E-6 | 8.433524E-5 |

FDM-SOR $\Delta t = \Delta x$

| No. of hx = hy cells | No. of iterations | CPU time (sec) | Max function error | Max derivative error |
|---|---|---|---|---|
| 8 | $8 \times 7 = 56$ $\omega = 1.55$ | 0.134 | 1.20095E-2 | 9.07367E-2 |
| 16 | $16 \times 20 = 320$ $\omega = 1.7$ | 3.4 | 3.21928E-3 | 5.0422E-2 |
| 32 | $32 \times 34 = 1088$ $\omega = 1.7$ | 49.85 | 8.3834E-4 | 2.16456E-2 |
| 64 | $64 \times 92 = 5888$ $\omega = 1.7$ | 1122.8 | 2.3626E-4 | 1.1279E-2 |

Table 1. Problem (a) $u(x, y, t) = \exp(t - x\cos\theta - y\sin\theta)$, $\theta = \pi/4$

FDM-ADI $\Delta t = (\Delta x)^2$

| No. of hx = hy cells | No. of iterations | CPU time (sec) | Max function error | Max derivative error |
|---|---|---|---|---|
| 8 | 32 | 0.2834 | 2.07583E-2 | 1.055968E-1 |
| 16 | 128 | 4.45 | 6.48407E-3 | 5.343229E-2 |
| 32 | 512 | 69.65 | 1.826602E-3 | 2.889879E-2 |
| 64 | 2048 | 1105.48 | 8.967522E-4 | 1.5545622E-2 |

CPT-ADI $\Delta t = \Delta x$

| No. of hx = hy cells | No. of iterations | CPU time (sec) | Max function error | Max derivative error |
|---|---|---|---|---|
| 8 | 8 | 0.15 | 9.359392E-5 | 1.9731343E-3 |
| 16 | 16 | 1.0 | 2.366787E-5 | 6.054254E-4 |
| 32 | 32 | 7.567 | 5.9340348E-6 | 2.120109E-4 |
| 64 | 64 | 58.8 | 1.4842674E-6 | 8.433524E-5 |

FDM-SOR $\Delta t = \Delta x$

| No. of hx = hy cells | No. of iterations | CPU time (sec) | Max function error | Max derivative error |
|---|---|---|---|---|
| 8 | $8 \times 7 = 56$ $\omega = 1.55$ | 0.134 | 1.20095E-2 | 9.07367E-2 |
| 16 | $16 \times 20 = 320$ $\omega = 1.7$ | 3.4 | 3.21928E-3 | 5.0422E-2 |
| 32 | $32 \times 34 = 1088$ $\omega = 1.7$ | 49.85 | 8.3834E-4 | 2.16456E-2 |
| 64 | $64 \times 92 = 5888$ $\omega = 1.7$ | 1122.8 | 2.3626E-4 | 1.1279E-2 |

Table 2. Problem (b) $u(x, y, t) = 2t + x^2 \cos^2\theta + y^2 \sin^2\theta$, $\theta = \pi/4$

FDM-ADI $\Delta t = (\Delta x)^2$

| No. of hx = hy cells | No. of iterations | CPU time (sec) | Max function error | Max derivative error |
|---|---|---|---|---|
| 8 | 32 | 0.4167 | 1.3274E-4 | 1.202978E-2 |
| 16 | 128 | 6.7667 | 5.55037E-5 | 6.083185E-3 |
| 32 | 512 | 110.28 | 2.80686E-5 | 3.063236E-3 |
| 64 | 2048 | 1786.05 | 1.39326E-5 | 1.538248E-3 |

CPT-ADI $\Delta t = \Delta x$

| No. of hx = hy cells | No. of iterations | CPU time (sec) | Max function error | Max derivative error |
|---|---|---|---|---|
| 8 | 8 | 0.1834 | 6.84861E-4 | 2.73903E-3 |
| 16 | 16 | 1.3167 | 3.521155E-4 | 1.408662E-3 |
| 32 | 32 | 10.267 | 1.780065E-4 | 7.121056E-4 |
| 64 | 64 | 80.834 | 8.942948E-5 | 3.57749E-4 |

FDM-SOR $\Delta t = \Delta x$

| No. of hx = hy cells | No. of iterations | CPU time (sec) | Max function error | Max derivative error |
|---|---|---|---|---|
| 8 | $8 \times 1 = 8$ $\omega = 1.7$ | 5.0E-2 | 2.802506E-3 | 1.842519E-2 |
| 16 | $16 \times 2 = 32$ $\omega = 1.9$ | 1.1334 | 1.089026E-3 | 1.286985E-2 |
| 32 | $32 \times 5 = 160$ $\omega = 1.85$ | 12.784 | 6.681835E-4 | 4.63165E-3 |
| 64 | $64 \times 16 = 1024$ $\omega = 1.9$ | 319.58 | 8.712826E-5 | 1.700953E-3 |

Table 3. Problem (c) $u(x, y, t) = x (1 - x) y (1 - y) e^{-t}$

**3. Concluding remarks.** The x, y domains are devided into 8, 16, 32 and 64 cells and in each case, the starting time is taken to be 0 and the final time is 1. The relation between time step and space step varies among FDM-ADI, FDM-SOR and CPT-ADI schemes. We assume all the material constants are equal to unity and $\Delta x = \Delta y$. In case of FDM-SOR and CPT-ADI, $\Delta x = \Delta y = \Delta t$ and however, in case of FDM-ADI, $\Delta t = (\Delta x)^2$. This is a disadvantage for FDM-ADI. For example, when Dx = 1.5625E-2, Dt = 4.883E-4 and it would take 2048 iterations to reach time 1. However, CPT-ADI and FDM-SOR are free from this difficulty. But SOR also has a different disadvantage. Each time step, FDM-SOR takes large number of iterations to converge to a preassigned level. With 64 cells CPT-ADI requires only 64 iterations to reduce the error level to 4.84303E-7, where as FDM-ADI requires 2048 iterations to educe the error level to 4.081723E-4 and FDM-SOR requires 5,952 iterations to reduce the error level to 7.7714E-6.

Perhaps the most convincing argument may be made in favor of CPT-ADI with respect to CPU times. In this respect, CPT-ADI is the best. With 64 cells, CPT-ADI requires only 58.8 secs where as FDM-ADI and FDM-SOR need 1105.48 secs and 1122.8 secs respectively to compute the same problem.

Acknowledgments: Thanks to Milton E. Rose for his many valuable suggestions for the completion of this paper. Also many thanks go to Arje Nachman of AFOSR.

## References

1. M. E. Rose, "Compact finite volume methods for the diffusion equations", J. Sci. Comp., vol 4, no. 3 (1989), pp. 261-290

ATTACHMENT #5

# Stefan 2D

This parer reports on the solution of the *Stefan* problem in 2 dimensions. The codes are written in *True Basic*, and the *Enthalpy* formulation of the 2D Stefan problem is approximated by *Compact* Schemes. The numerical results are compared to an exponential solution, and the solution and errors are plotted using *Mathematica*.

## Dirichlet boundary conditions

The following results pertain to an exponential solution of the Stefan problem. The melting front moves on lines $t - x\cos\theta - y\sin\theta = \kappa$ with speed 1.

$$\Theta = 0$$

The parameters set in the code specified 32 cells in all directions, and solution in [0, .7] time interval. The problem is reduced to 1D.

### Import data

### Plot Data

A contour plot of the analytic solution would reveal horizontal lines behind the front at position 22.4. Below is the contour plot of the numerical solution.

```
ListContourPlot[C1, PlotLabel->"Temperature",
ContourLevels->20]
```

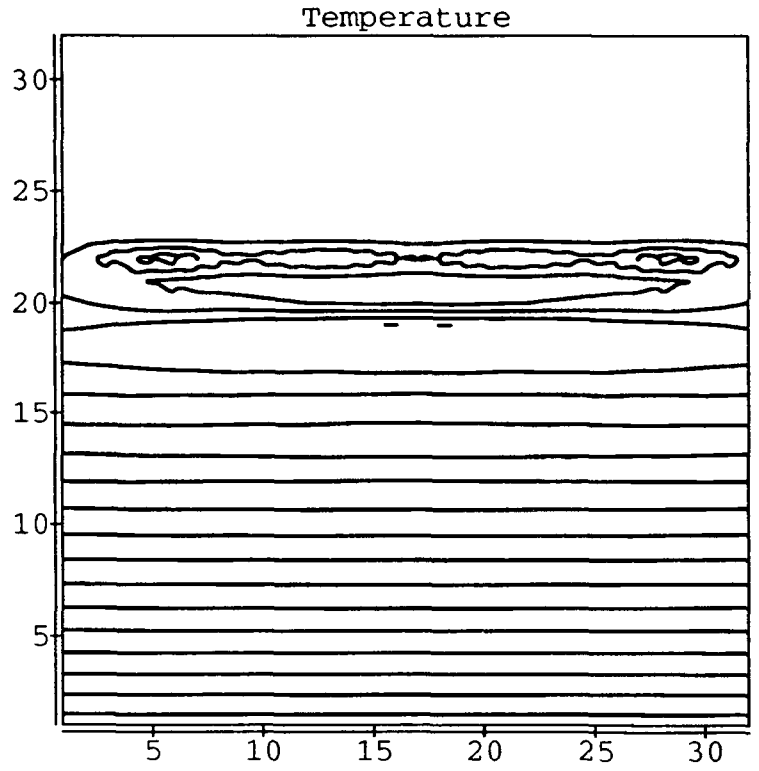


-ContourGraphics-

**A 3D plot of the numerical solution shows the behaviour in the neighborhood of the front.**

```
ListPlot3D[S1, PlotLabel->"Temperature", Shading->False,
ViewPoint->{4.000, 0.910, 1.290}]
```

Temperature

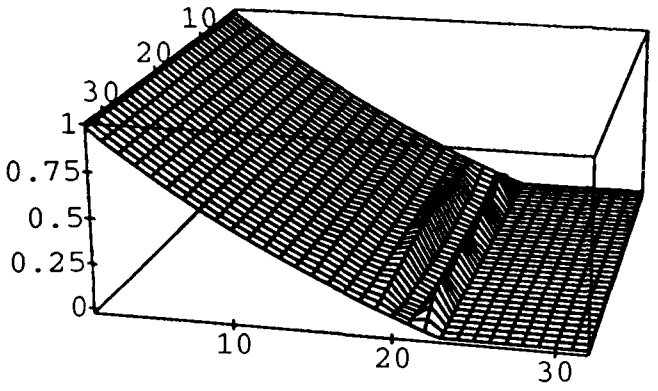


-SurfaceGraphics-

**Below is a plot of the positions of the numerical front for each corresponding time frame.**

```
ListPlot3D[F1, PlotLabel->"Front tracking", Shading->False,
ViewPoint->{0.790, -2.570, 1.290}]
```

Front tracking

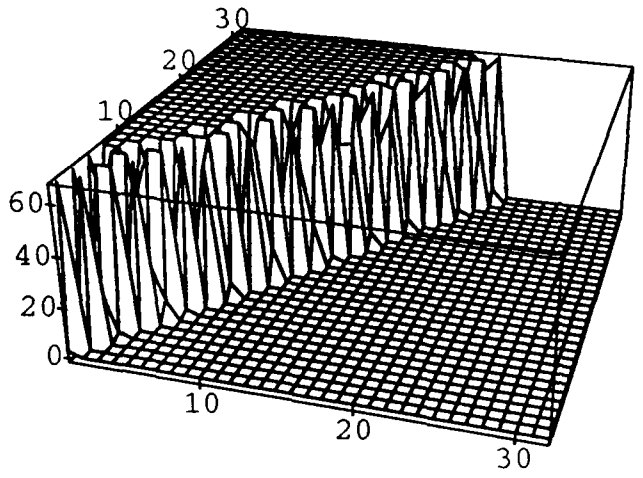


-SurfaceGraphics-

**A 3D plot of the numerical error shows that it is mostly confined to the neighborhood of the front.**

```
ListPlot3D[E1, PlotLabel->"Error", Shading->False,
PlotRange->All, ViewPoint->{4.000, 0.910, 1.290}]
```

Error

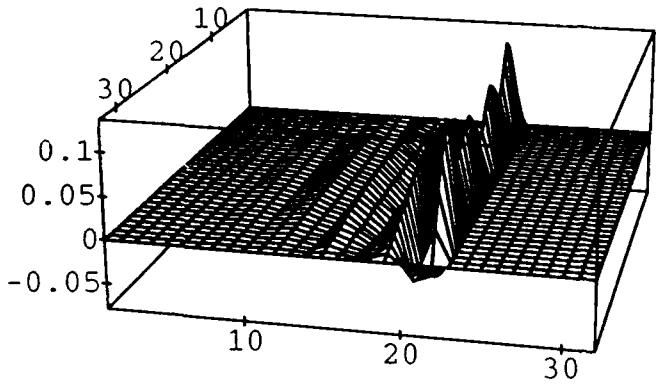


-SurfaceGraphics-

$$\Theta = \pi/4$$

The parameters set in the code specified 32 cells in all directions, and solution in [0, .7] time interval.

## Import data

## Plot Data

A contour plot of the analytic solution would reveal diagonal lines behind the front. Below is the contour plot of the numerical solution.

```
ListContourPlot[C2, PlotLabel->"Temperature",
ContourLevels->20]
```

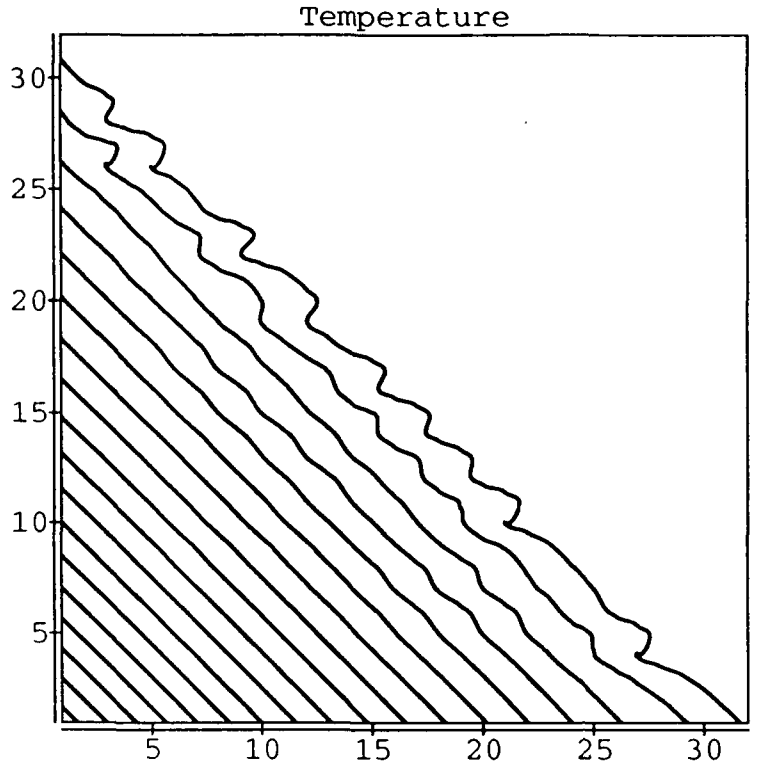


-ContourGraphics-

**A 3D plot of the numerical solution shows the behaviour in the neighborhood of the front.**

```
ListPlot3D[S2, PlotLabel->"Temperature", Shading->False,
ViewPoint->{4.000, 0.910, 1.290}]
```

Temperature

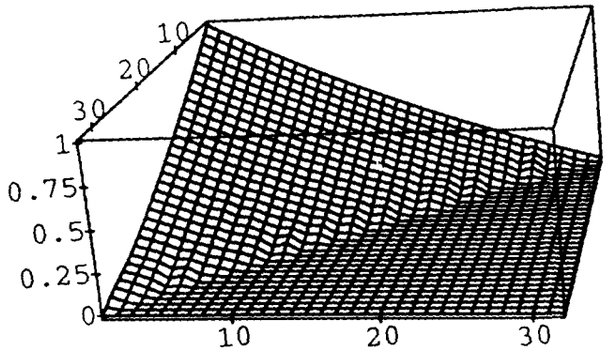


-SurfaceGraphics-

**Below is a plot of the positions of the numerical front for each corresponding time frame.**

```
ListPlot3D[F2, PlotLabel->"Front tracking", Shading->False,
ViewPoint->{0.790, -2.570, 1.290}]
```

Front tracking

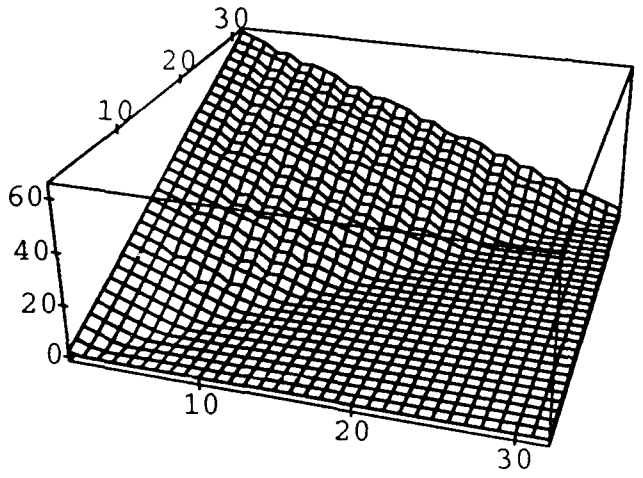


-SurfaceGraphics-

**A 3D plot of the numerical error shows that it is mostly confined to the neighborhood of the front.**

```
ListPlot3D[E2, PlotLabel->"Error", Shading->False,
PlotRange->All, ViewPoint->{4.000, 0.910, 1.290}]
```

Error

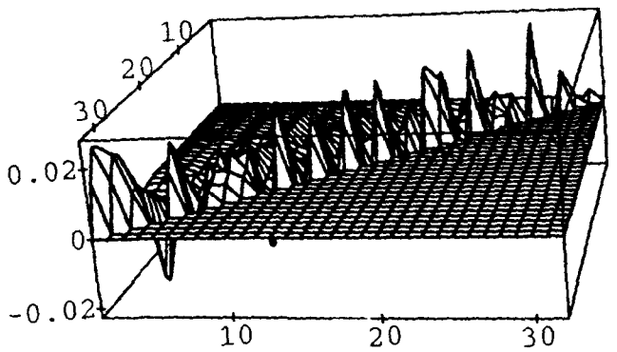


-SurfaceGraphics-

# Neumann boundary conditions

The following results pertain to an exponential solution of the Stefan problem. The melting front moves on lines $t - x\cos\theta - y\sin\theta = \kappa$. This code uses flux boundary conditions.

## Left + Lower Flux boundary conditions

■ $\Theta = 0$

■ $\Theta = \pi/4$

The parameters set in the code specified 32 cells in all directions, and solution in [0, .7] time interval.

■ Import data

## Plot Data

**Below is the contour plot of the numerical solution.**

```
ListContourPlot[C4, PlotLabel->"Temperature",
ContourLevels->20]
```

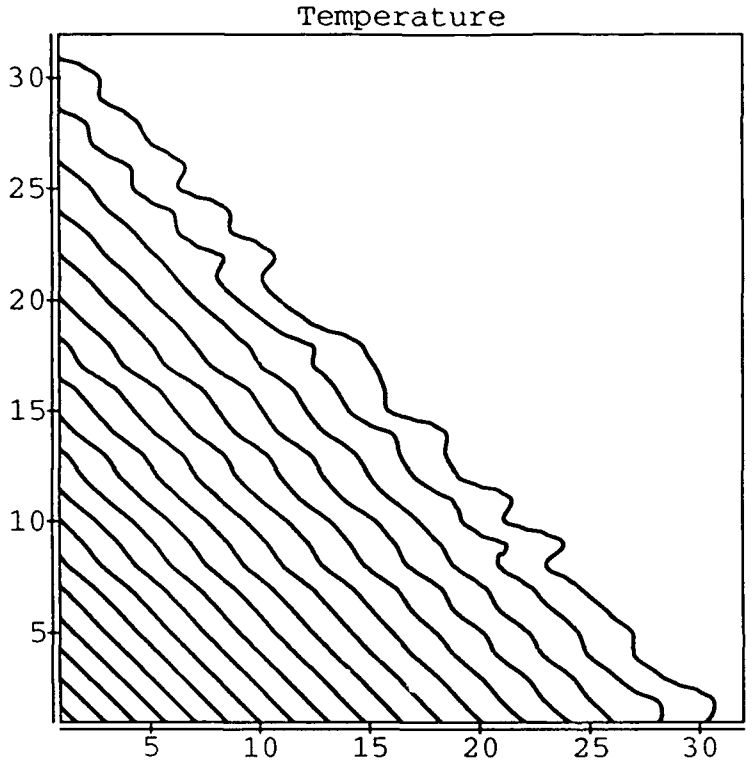


-ContourGraphics-

**A 3D plot of the numerical solution shows the behaviour in the neighborhood of the front.**

```
ListPlot3D[S4, PlotLabel->"Temperature", Shading->False,
ViewPoint->{4.000, 0.910, 1.290}]
```

Temperature

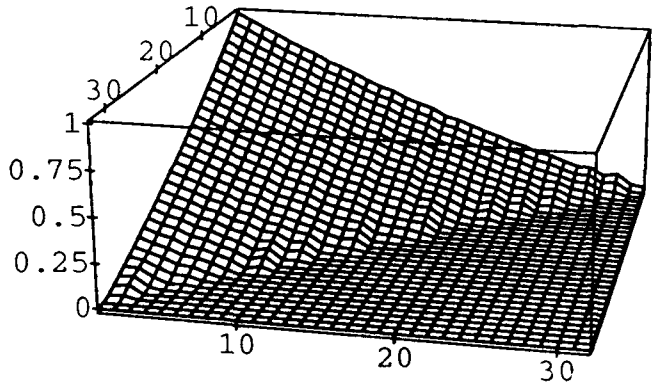


-SurfaceGraphics-

**Below is a plot of the positions of the numerical front for each corresponding time frame.**

```
ListPlot3D[F4, PlotLabel->"Front tracking", Shading->False,
ViewPoint->{0.790, -2.570, 1.290}]
```

Front tracking

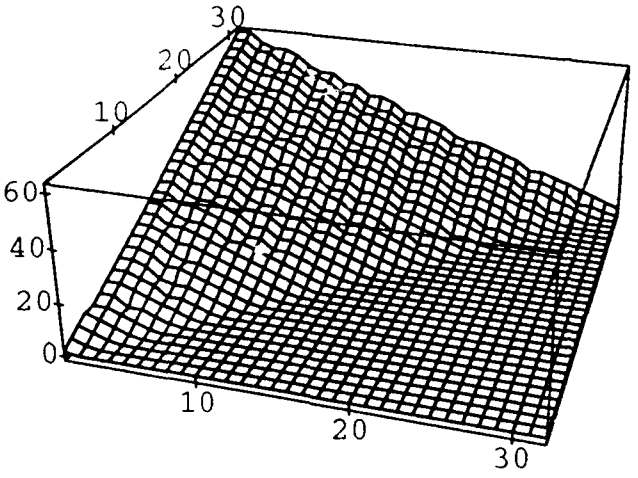


-SurfaceGraphics-

**A 3D plot of the numerical error shows that it is mostly confined to the neighborhood of the front.**

```
ListPlot3D[E4, PlotLabel->"Error", Shading->False,
PlotRange->All, ViewPoint->{4.000, 0.910, 1.290}]
```

Error

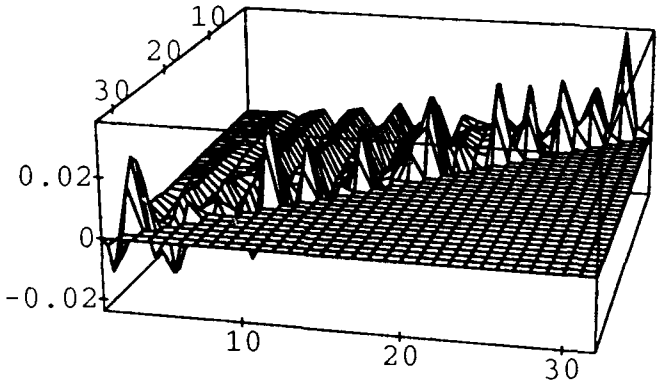


-SurfaceGraphics-

## All Flux boundary conditions

■ $\Theta = 0$

■ $\Theta = \pi/4$

The parameters set in the code specified 32 cells in all directions, and solution in [0, .7] time interval.

## ■ Import data

## ■ Plot Data

Below is the contour plot of the numerical solution.

```
ListContourPlot[C6, PlotLabel->"Temperature",
ContourLevels->20]
```

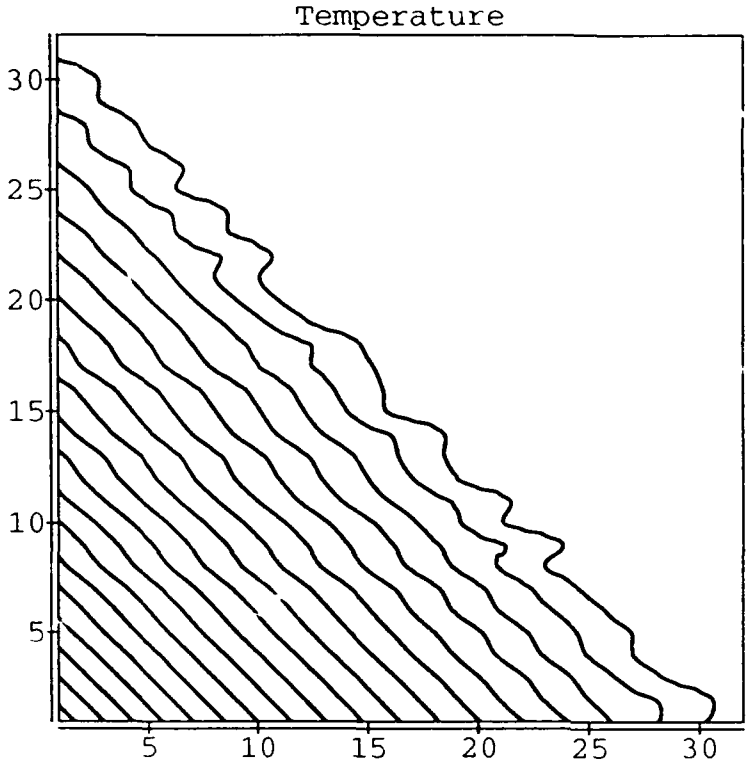


-ContourGraphics-

**A 3D plot of the numerical solution shows the behaviour in the neighborhood of the front.**

```
ListPlot3D[S6, PlotLabel->"Temperature", Shading->False,
ViewPoint->{4.000, 0.910, 1.290}]
```

Temperature

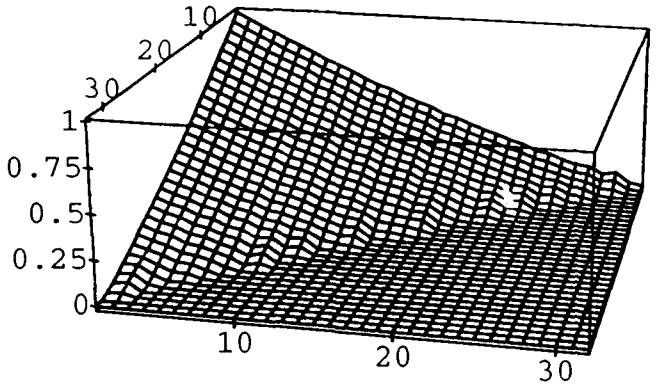


-SurfaceGraphics-

**Below is a plot of the positions of the numerical front for each corresponding time frame.**

```
ListPlot3D[F6, PlotLabel->"Front tracking", Shading->False,
ViewPoint->{0.790, -2.570, 1.290}]
```

Front tracking

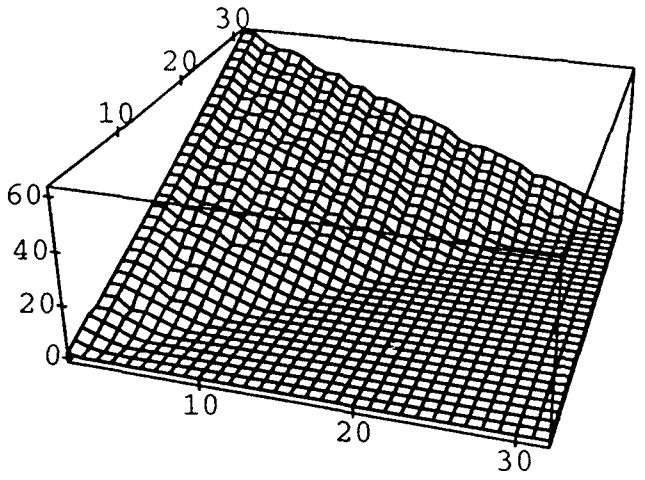


-SurfaceGraphics-

**A 3D plot of the numerical error shows that it is mostly confined to the neighborhood of the front.**

```
ListPlot3D[E6, PlotLabel->"Error", Shading->False,
PlotRange->All, ViewPoint->{4.000, 0.910, 1.290}]
```

Error

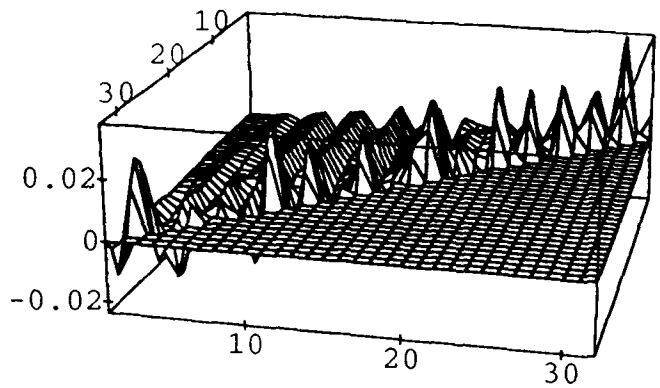


-SurfaceGraphics-